

# Poly(Vinyl Alcohol) Cryogels for Biomedical Applications

Wankei Wan, A. Dawn Bannerman, Lifang Yang, and Helium Mak

## Contents

1	Introduction .....	285
2	Processing Parameters for PVA-C Preparation .....	285
2.1	Molecular Weight .....	286
2.2	Solution Concentration .....	287
2.3	Solvent .....	288
2.4	Freeze–Thaw Cycling .....	288
3	Properties of PVA and PVA Composites .....	290
3.1	Mechanical Properties .....	290
3.2	Diffusion Characteristics .....	298
4	PVA Composite Cryogels .....	302
4.1	Cellulose-PVA Composites .....	302
4.2	Chitosan-PVA Composites .....	304
5	Biomedical Applications .....	306
5.1	Medical Devices .....	306
5.2	PVA-C Tissue Hybrid .....	311
6	Future Perspectives .....	314
	References .....	316

**Abstract** Poly(vinyl alcohol) (PVA) is a hydrophilic and biocompatible polymer that can be crosslinked to form a hydrogel. When physically crosslinked using a freeze–thaw cycling process, the product hydrogel or cryogel (PVA-C) possesses

---

W. Wan (✉)

Graduate Program in Biomedical Engineering, University of Western Ontario, London, ON, Canada N6A5B9

Department of Chemical and Biochemical Engineering, University of Western Ontario, London, ON, Canada N6A5B9

e-mail: [wkwan@uwo.ca](mailto:wkwan@uwo.ca)

A.D. Bannerman • L. Yang • H. Mak

Graduate Program in Biomedical Engineering, University of Western Ontario, London, ON, Canada N6A5B9

unique mechanical properties that can be tuned to closely match those of soft tissues, thus making it an attractive candidate for biomedical and especially medical device applications. We review the freeze–thaw cycling process and processing parameters that impact on the properties of PVA-C and its nanocomposite products. Both the mechanical properties and diffusion properties relevant to biomedical application are discussed. Applications to orthopedic and cardiovascular devices are summarized and discussed. The concept of biomaterial–tissue hybrids that can impart the necessary hemocompatibility to PVA-C for cardiovascular device is introduced and demonstrated.

**Keywords** Poly(vinyl alcohol) • Physical crosslinking • Cryogel • Medical device • Controlled release

### List of Abbreviations

BC	Bacterial cellulose
BSA	Bovine serum albumin
DMSO	Dimethyl sulfoxide
DP	Degree of polymerization
$E'$	Young's modulus
FITC	Fluorescein isothiocyanate
FT	Freeze–thaw
FTC	Freeze–thaw cycle
WIC	Water insoluble chitosan
IVD	Intervertebral disc
Nano-HA	Nanohydroxyapatite
NP	Nucleus pulposus
PAAm	Poly(acrylamide)
PEG	Poly(ethylene glycol)
PVA	Poly(vinyl alcohol)
PVA-C	Poly(vinyl alcohol) cryogel
PVA-BC	Poly(vinyl alcohol) bacterial cellulose composite
PVP	Polyvinyl pyrrolidone
RGD	Arginyl-glycyl-aspartic acid
SANS	Small-angle neutron scattering
TEM	Transmission electron microscopy
UHMWPE	Ultrahigh molecular weight polyethylene
ULMP	Unfrozen liquid microphase
WSC	Water-soluble chitosan

## 1 Introduction

Polyvinyl alcohol (PVA) is a hydrogel with desirable properties for biomedical applications [1, 2]. Ivalon™, a highly porous PVA sponge crosslinked with formaldehyde, was probably one of the first medical products marketed [3]. It was used extensively in duct replacement, articular cartilage replacement [4], as a pharmaceutical release agent [1], and in reconstructive (vocal cord) surgery [5]. In addition to the use of chemical crosslinking agents such as formaldehyde and glutaraldehyde, PVA can also be crosslinked using several other methods, such as the use of electron beam,  $\gamma$ -irradiation, and physical crosslinking. For biomedical applications, physical crosslinking has the advantage of not leaving residual amounts of toxic crosslinking agents, as well as providing higher and more tunable mechanical strength than the PVA gels crosslinked by either chemical or irradiative techniques [6]. The physical crosslinking methods have generated the most interest because no new chemicals are introduced that could complicate their use in the biomedical environment.

Physical crosslinking can be accomplished using a freeze–thaw (FT) cycling method in which a solution of PVA is allowed to undergo repeated freezing and thawing cycles. For obvious reasons, the product hydrogel is popularly called a PVA cryogel (PVA-C). Using this approach, and by carefully controlling the process parameters used in the hydrogel preparation procedure, material properties, including mechanical and diffusion properties, can be tailored. Moreover, with the incorporation of nanomaterials into the PVA solution, nanocomposites of interesting mechanical properties (tensile and compressive) relevant to a range of medical device applications can be created. We will focus on the preparation and properties of PVA-C and its composites by the freeze–thaw method. Biomedical applications in the areas of medical device and drug delivery will be used to illustrate the range of biomedical applications possible for this class of hydrogel material.

## 2 Processing Parameters for PVA-C Preparation

PVA-C is today one of the most commonly investigated cryogels for biomedical applications. PVA, which is synthesized through hydrolysis of polyvinyl acetate synthesized via free radical polymerization of vinyl acetate [6], consists of a secondary alcohol group attached to a linear carbon chain. The alcohol group allows for hydrogen bonding and, therefore, PVA dissolved in an aqueous solution is able to produce a hydrogel with high water content. Subsequent thermal cycling leads to physical crosslinking via formation of structured crystalline domains of the polymer chains through phase separation. Several phases occur during the thermal cycling process. First, the gel is brought down to a temperature of between  $-5$  and  $-20$  °C [7], during which time the water phase freezes. This creates regions of high polymer concentration, where crystallites are formed, as well as regions of low

polymer concentration resulting in pores [8–10]. The solution is then thawed back to room temperature leading to the formation of a solid gel—PVA-C. The micro-/nanostructure of PVA-C has been examined through several techniques including transmission electron microscopy (TEM) [9], small angle X-ray scattering (SAX) [9] and small angle and ultrasmall angle neutron scattering (SANS and USANS) [10, 11]. Observations conclude that the first freeze–thaw cycle (FTC) produces polymer-rich regions due to the formation of ice crystals in the amorphous regions [10, 12]. Subsequent FTCs further modify the structure of the polymer matrix.

Formation of the PVA-C takes place during the thawing stages [13]. Crystallization and phase separation are two important mechanisms that contribute to the structure of PVA-C, with crystallization occurring in the first three FTCs and phase separation through at least six cycles. Phase separation has a very important impact on the mechanical properties of PVA, even apart from crystallization [14].

A range of parameters in the processing procedures for PVA cryogels can be modified to alter the structure and properties of PVA-C and therefore its application. Polymer molecular weight and PVA solution concentration both have significant effects on structure [7, 12, 15–17]. The conditions of the FTCs, such as freezing and thawing rate, number of FTCs, and upper and lower temperature limits, all contribute to the determination of polymer matrix structure [7]. This wide range of processing parameters provides alternatives for tuning the properties of PVA cryogels. This is extremely beneficial because it makes the material useful for a large number of applications, and precise adjustments can be made to tailor the material for a specific application.

Significant work has been reported on how the Young's modulus of PVA cryogel is affected by processing parameters [7]. Work by Pazos et al. studied the nonlinear elastic response of PVA cryogel under uniaxial tension. The authors found that varying the number of cycles and the thawing rate could have similar effects on the elastic modulus, but changing the thawing rate gave finer control. Gels processed under specific conditions were found to mimic the uniaxial elastic response of healthy porcine coronary arteries [18]. Studies by our group using SANS were able to show that anisotropic mechanical properties can be achieved for PVA cryogels through processing the gel under controlled applied stress. This is extremely beneficial for biomedical devices such as coronary bypass grafts, where the tissue being replaced possesses orientational-dependent mechanical properties [10].

## ***2.1 Molecular Weight***

Molecular weight has a significant effect on PVA-C formation [19]. As molecular weight increases, the number and size of the crystalline regions increases due to the increase in length of the polymer chain. However, this effect is limited by the decrease in free volume and mobility of the high molecular weight polymers. Hassan and Peppas found that during swelling there was more instability in crystal

uniformity and degree of crystallinity in the higher molecular weight PVA due to an increase in chain length. This contributes to additional crystallization during swelling and increased mobility because of less physical crosslinking, as indicated by higher overall volume swelling ratio.

Lozinsky et al. found that gels produced with a lower molecular weight were more rigid than those of a higher molecular weight, up to a maximum. The unfrozen liquid microphase (ULMP), specific to cryotropic gelation, is important in explaining this phenomenon. The viscosity of the ULMP is highest in the system with the highest molecular weight polymer because the polymers have the longest chain length. This decreased mobility reduces intermolecular interactions. Therefore, although the rigidity normally increases as polymer molecular weight increases, a build-up in ULMP viscosity limits this increase [20].

The ability to change the degree of crystallinity by adjusting molecular weight is an important factor for biomedical applications. Degree of crystallinity has an effect on the mechanical properties and diffusion properties. For example, PVA-C can be tuned in this way to achieve mechanical properties that mimic tissue ranging from cardiovascular tissue to skin [7].

## 2.2 Solution Concentration

Initial PVA solution concentration was studied as one of the first processing parameters that can be altered to affect the structure and properties of PVA-C. Trieu and Qutubuddin showed that many processing parameters have an effect on the structure and mechanical properties of PVA cryogels, including initial PVA concentration. They found that a higher initial PVA concentration produces a structure with less porosity. This, in turn, lowers the equilibrium swelling, resulting in an inverse relationship between equilibrium swelling and porosity [21].

Hassan and Peppas varied the PVA solution concentration and noted that the higher concentration solutions resulted in more stable gels that have higher degrees of crystallinity and lower secondary crystallization. Lower degrees of swelling in higher concentration solutions indicate that more crosslinking occurs in higher concentration solutions [19].

Lozinsky et al. demonstrated that an increase in PVA concentration results in an increase in cryogel rigidity. This is due to the increased concentration of hydroxyl groups present, creating an increase in intermolecular hydrogen bonding. This factor was also determined to be more effective in controlling the properties than the effect of ULMP viscosity previously described. Furthermore, as polymer concentration is increased, porosity decreases and a more ordered structure results [20].

An increase in the concentration of PVA has been shown to produce more crystalline structures with greater stability. This, in turn, causes an increase in the tensile strength and tear resistance [22]. Wan et al. found that an increase in the PVA concentration caused the stiffness of PVA-C to increase significantly. With an

increase in PVA concentration from 10 % to either 15 or 20 %, the tangent elastic modulus increased by 69 and 137 %, respectively, and the secant elastic modulus increased by 83 and 180 %, respectively, at a strain of 0.25 [23].

### 2.3 Solvent

The use of different solvents in the processing of PVA can dramatically alter the PVA-C properties. Hassan and Peppas have reviewed this area well [6]. Hyon and Ikada showed that the use of organic solvents such as dimethyl sulfoxide (DMSO), glycerin, ethylene glycol, propylene glycol, and ethyl alcohol provides excellent light transmittance, along with good tensile strength and high water content, making a gel material with good potential for contact lens applications [24]. The addition of DMSO has been studied extensively because it imparts transparency to the PVA-C. Ohkura et al. showed that DMSO/water solutions with PVA exhibit transparency, high elasticity and higher gelation rates because gelation occurs without phase separation at temperatures below  $-20\text{ }^{\circ}\text{C}$  [25]. Murase et al. showed that crystallinity increased over time due to the interaction between water and DMSO in the PVA-C [6].

Additives are sometimes put into the PVA solution. Lozinsky et al. showed that by adding triethylene glycols and its higher oligomers, the strength and thermal stability of the PVA cryogels increased and the gelation process was altered [26, 27].

For biomedical applications, the presence of salts or other solutes in the environment while producing PVA-C can be beneficial because the biomaterial will eventually be used in an electrolyte-containing physiological environment. Due to freezing point depression as a result of increased solute concentration, the freezing point of PVA solution decreases with the addition of salts. Gordon showed that the freezing point of PVA in water was  $-18.7\text{ }^{\circ}\text{C}$  [28], whereas Shaheen et al. demonstrated a decrease of freezing point to  $-30\text{ }^{\circ}\text{C}$  when PVA, theophylline, and 11 % NaCl was used [29]. The intermolecular and intramolecular hydrogen bonds that are so important to the formation of crystallites in PVA-C are disrupted by the presence of salts [30]. The crystallinity of PVA-C was shown to decrease and the cryogel became weaker when prepared in the presence of NaCl (0.0125–0.0625 M) compared to when distilled water was used [31].

### 2.4 Freeze–Thaw Cycling

As described above, the freeze–thaw cycling process allows the formation of amorphous and crystalline regions to form a physically crosslinked matrix of PVA. The number of FTCs, rate of freezing and thawing, and the time for which the gel is held frozen (freezing holding time) all have direct impact on the structure

of the resulting cryogel. For example, with an increase in the number of FTCs, there is a decrease in pore size within the polymer matrix [8, 32], an increase in mechanical properties [7] and a decrease in diffusion rates (see Sect. 3.2). An increase in freezing rate has been shown to decrease the size and density of crystallites. The freeze–thaw process is reviewed here in terms of its effect on PVA-C for applications in biomedicine.

#### 2.4.1 Rate of Freeze–Thaw Cycles

The rate of the thermal cycles has been shown to affect the mechanical properties of the PVA hydrogel. A stiffer material is produced by using a slower thawing rate because of the increased amount of time for the reorganization of polymer chains and squeezing out of water molecules. Hatakeyama et al. showed that the rate of freezing affects the size of the crystals and, therefore, the number of crystals formed [33]. Slower thawing increases the period in which the specimen is at temperatures optimal for gel network formation [13].

Lozinsky et al. found that the more time that the solution spends at temperatures below 0 °C, the more time is available for movement of polymer chains. This allows for more time for entanglements to occur and increases the crystallinity by increasing both the number and size of crystallites [34]. This produces PVA-C with increased tensile strength. The rate of freezing has less of an effect on the properties, but has been shown to affect the formation of ice crystals [33]. Thawing rates, on the other hand, affect the formation of the PVA-C and its mechanical properties [7, 18, 35, 36].

It is important to keep thawing rates below 10 °C/min, as higher rates are not acceptable for producing hydrogels [35]. In many studies, precise control of freezing and thawing rates are not maintained because samples are simply placed in a freezer for freezing and then removed to room temperature for thawing [37–39]. This will still result in cryogel formation, but the structure, and therefore the properties, of the PVA-C will not be reproducible.

#### 2.4.2 Number of Freeze–Thaw Cycles

In work by Hassan et al., the amount of dissolution of PVA cryogels was shown to decrease as the number of FTCs was increased [40]. This is consistent with the results that each FTC after the second causes a significant increase in the degree of crystallinity [37, 41].

It has been shown that the number of FTCs has an effect on mechanical properties. A maximum number of FTCs, after which the structure and properties of the cryogel no longer changes, has been demonstrated [8], and several studies have found this maximum number to be six [39, 42]. The increase in PVA-C stiffness with increasing number of FTCs has been attributed to the crystallite formation mechanism and liquid–liquid phase separation [7]. An alternative

explanation is the reinforcement of additional existing crystals within the structure with each additional FTC, up to a maximum level [19, 34].

### 2.4.3 Freeze Holding Time

The freezing holding time has a significant effect, with samples frozen up to 10 days at  $-10\text{ }^{\circ}\text{C}$  giving the most mechanically strong PVA hydrogels [34]. On the other hand, holding the sample at a lower temperature for varying amounts of time did not seem to have an effect on the mechanical properties. Wan et al. showed that holding times of 1 or 6 h at  $-20\text{ }^{\circ}\text{C}$  did not cause any change in the tensile properties of the PVA hydrogel [7]. Nevertheless the lower temperature limit, at which the hydrogel freezes, has an effect on the phase equilibrium of PVA, with storage of frozen solutions at higher negative temperatures resulting in PVA-C that is to some extent more rigid [21].

## 3 Properties of PVA and PVA Composites

### 3.1 Mechanical Properties

PVA cryogel (PVA-C) has caught the interest of researchers in the biomedical field since its creation in the early 1980s [43]. Apart from its long-term biocompatibility and nontoxicity [44], its mechanical properties, which can be tailored to mimic a wide range of soft tissues [7, 45], are the main reason why PVA-C is an attractive candidate material for many prosthetic devices such as heart valves, blood vessels, and articular cartilages.

In terms of mechanical strength (compressive or tensile), PVA-C can be isotropic or anisotropic [10]. Its Young's modulus is nonlinear and dependent on strain, strain rate, and temperature [46]. It is viscoelastic and strongly hydrophilic. Its strength is a function of concentration of the PVA solution, the mean molecular weight of the polymer material, the number of FTCs it has gone through during its formation, post-hydration processing, the type of buffer solution, and the solution temperature.

To understand the mechanical properties of PVA-C, one has to understand the microstructure of the cryogel, which is a direct result of its formation process. Although the gelation mechanism is still under discussion, it is thought to be a combination of mechanisms involving hydrogen bonding [47], crystallite formation, and liquid-liquid phase separation through spinodal decomposition [48].

Willcox et al. proposed a gelation scheme in support of the above hypothesis. When a PVA solution is subjected to a number of FTCs, during the first freezing cycle, ice crystallizations cause the remaining polymer solution to concentrate, bringing the molecular chains closer together. This promotes PVA crystallite

formation between the ice crystals. Inter- and intramolecular hydrogen bonds are also formed that connect the crystallites together and create an amorphous polymer network. Thawing of the ice crystals leaves behind regions of low polymer concentration solutions. Subsequent FTCs will repeat the process, reinforcing the PVA crystallites and tying up an increasing amount of the PVA molecules in the solution. At the end of the process, the final thawing of the ice crystals leaves behind micropores in the hydrogel body that are filled with the original solvent, typically water [9].

The structure of PVA hydrogels by repeated freezing and thawing cycles has been studied by several groups and the consensus is that they consist of a polymer-rich region and a polymer-poor region, which is consistent with Willcox's model [8, 10, 12, 15, 49, 50].

Based on micro-/nanodimension characterization, several structural models have been proposed [8, 9, 32]. One of the most recent and up-to-date studies used SANS. It was determined that the PVA-C structure consists of polymer crystallites of ~3 nm in size dispersed in the polymer-rich region with a spacing of ~19 nm between them [10]. During thawing, melting ice crystals create water-filled micrometer-sized macropores that make up the polymer-poor regions. The structural evolution during the FT process is illustrated in Fig. 1a.

Interestingly, the FT process can be altered by adding one additional step to the freeze-thaw procedure to create anisotropic PVA-C with orientation-dependent mechanical properties. Since most natural tissues are anisotropic in structure and properties, it is beneficial to be able to achieve this with polymer materials for tissue replacement applications. Millon et al. produced the first PVA-C flat sheet and conduit displaying anisotropic mechanical behavior similar to that of the porcine aorta. Structural anisotropy was created by applying an orientational-specific strain to the PVA sample after the initial FTC, and performing further thermal cycling on it. It was suggested that the applied strain forces the polymer mesh and polymer-poor phase to elongate in the direction of the strain. Subsequent FTCs then produce ice crystals that freeze and thaw in the strained pores that are already present, reinforcing the structure in the direction the strain is applied. The pores semi-oriented in the direction of strain can increase in size with the additional cycling. Additional crosslinking can also occur [10]. Figure 1b shows a model constructed on the basis of the SANS data.

The unique poro-viscoelastic mechanical property of PVA-C when subjected to external forces has been modeled using the finite element method. It has been shown to be a direct result of the part-solid and part-liquid biphasic structure [51]. This result is consistent with the model shown in Fig. 1b.

As the number of FTCs increases, the network mesh becomes denser and, hence, the strength of the PVA-C increases with the number of FTCs. However, after seven cycles, all available PVA materials in the initial solution are tied up in the mesh and the mechanical strength of PVA-C levels off [45].

As the initial concentration of the PVA solution increases, more polymers are available for network formation. The crystallinity increases and the polymer mesh becomes denser, but the pore size becomes smaller [23]. The denser polymer mesh

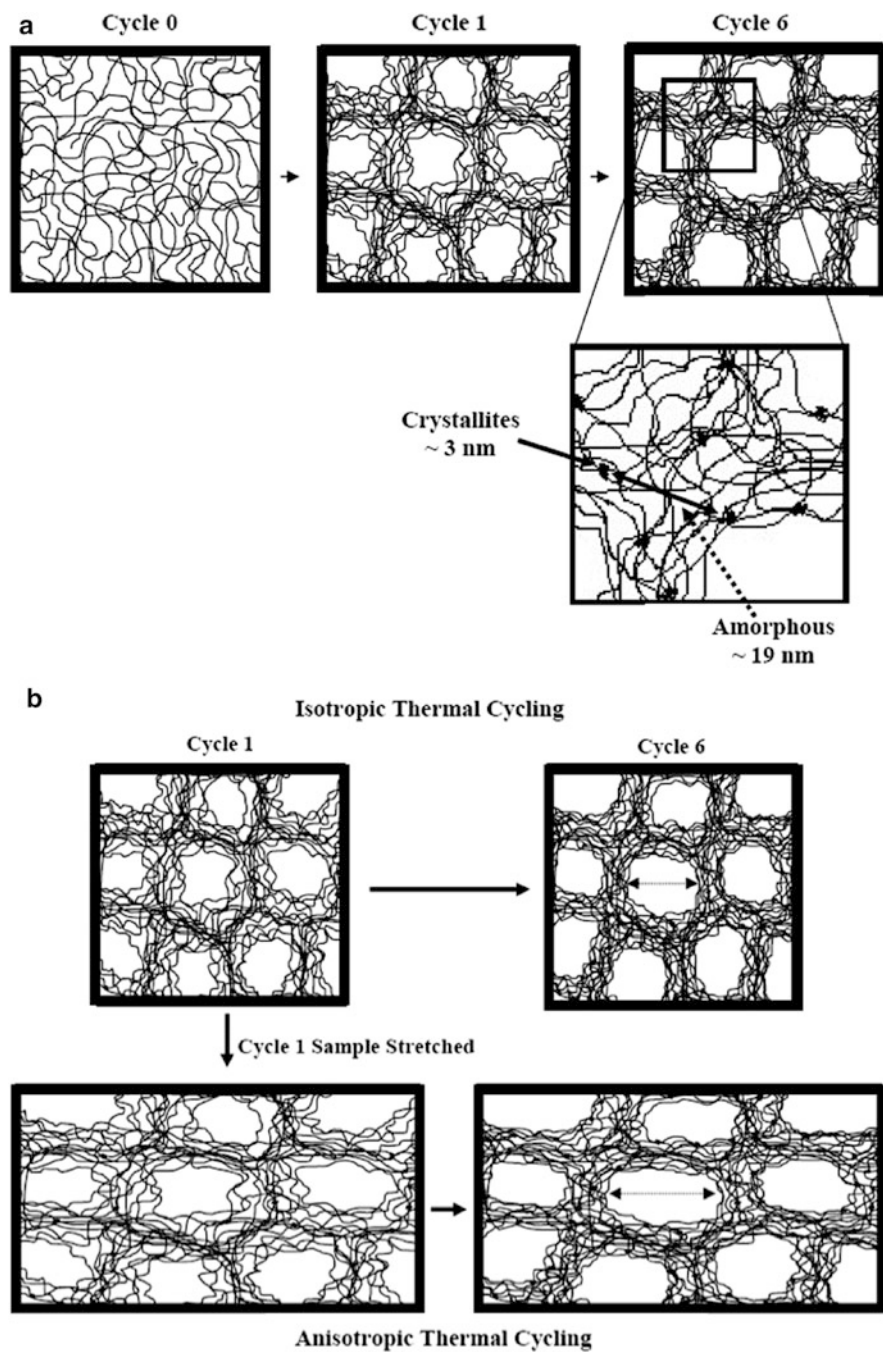


**Fig. 1** (a) Effect of freeze–thaw cycles on the microstructure of PVA. (b) Effect of initial strain and freeze–thaw cycles in production of anisotropic PVA-C. Reprinted from [10] with permission. Copyright (2007) American Chemical Society

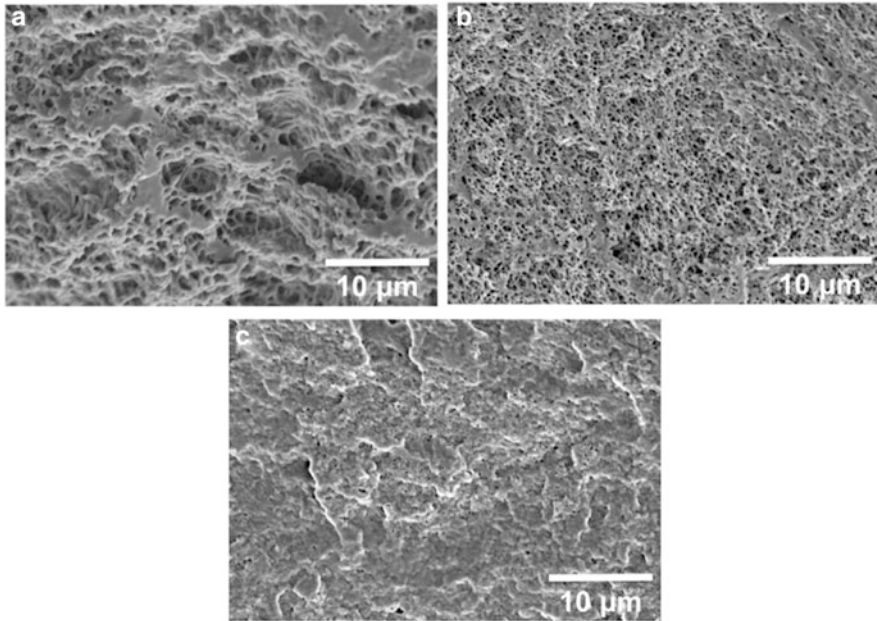


**Fig. 2** SEM images of fractured cross-sections of critical point dried PVA-C of different initial concentrations: (a) 10 %, (b) 15 %, and (c) 20 %. Reprinted from [23]

increases the strength of the PVA-C. Figure 2 shows the effect of increasing initial PVA concentrations on the pore size of the PVA-C [23]. Willcox et al. used cryo-TEM to measure the pore size of 19 wt% PVA-C after 12 FTCs to be  $\sim 30$  nm [9]. Nakaoki and Yamashita used thermodynamic equations to derive the pore size of 10 wt% PVA-C to be 30.2 nm [52].

Medical devices, depending on the physiological environment surrounding them, can be subjected to either compressive or tensile stress. Typical characterizations of the mechanical properties of a polymer material involve the measurements of its stress–strain curves, stress relaxation curves, and creep curves.

### 3.1.1 Compressive

The musculoskeletal system is a compressive stress environment. Any medical device in this system will operate under a state of compression. Compressive mechanical properties can be experimentally measured in either confined or unconfined conditions. Due to the porous nature of tissue, most experiments are carried out under unconfined conditions, in which the sample is compressed using nonporous platens and is allowed to expand at the circumferential direction without restrictions.

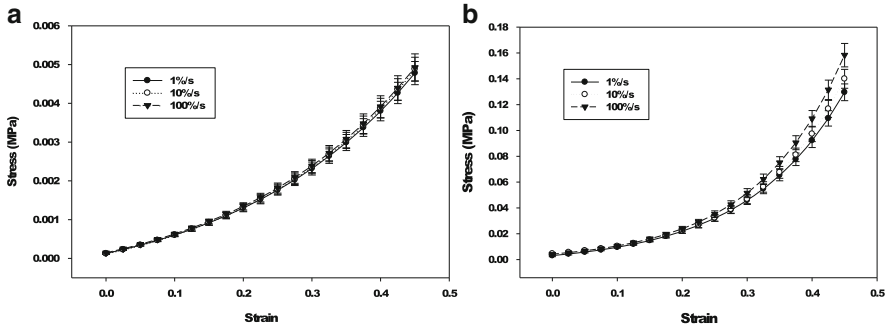


**Fig. 3** Effect of strain rate on 10 % PVA of (a) one and (b) six FTCs. Reprinted from [45] with permission. Copyright © 2009 Wiley Periodicals

Stammen et al. performed unconfined compression on samples made from two formulations of Salubria, which is a commercial cryogel of PVA and 0.9% saline (but the number of FTCs were not specified in the paper), containing 80 wt% water ( $\sim 20$  wt% PVA) and 75 wt% water ( $\sim 25$  wt% PVA). They measured the Young's modulus and the compressive failure of the samples in 37 °C deionized water using a compressive ramp to 65 % at a strain rate of 100 %/min (1.67 %/s) and 1,000 %/min (16.67 %/s). Their objective was to mimic the physiological conditions of articular cartilage. The authors found that the compressive mechanical properties of Salubria were significantly affected by strain and strain rate, exhibiting nonlinear viscoelastic behavior [53]. At strains less than 40 %, the Young's modulus of the 25 wt% was consistently higher than the 20 wt% samples, irrespective of material strain rate; however, the trend reversed above 60 % strain. At 30 % strain, a strain rate increase from 100 to 1,000 %/min had a strong effect on the 25 % samples but not on the 20 % samples. The compressive Young's modulus for the 20 % and 25 % samples were 0.7–6.8 MPa (at a strain rate of 100 %/min) and 1.1–18.4 MPa (at strain rate of 1,000 %/min), respectively. The compressive failure for the 20 % and the 25 % samples were found to be around 45 % strain at 1.4 MPa stress and 60 % strain at 2.1 MPa stress, respectively [53].

Millon et al. performed unconfined compressive tests on 10 wt% PVA-C samples through 1, 3, and 6 FTCs. The samples were tested using strain-rates of 1, 10, and 100 %/s at 0–45 % strain at 37 °C to mimic the physiological conditions of cartilage. Figure 3 shows the strain-rate dependency of 10 % PVA at 1 and 6 FTCs. The authors concluded that PVA-C exhibits the same exponential characteristic in stress–strain behavior as cartilage. However, it has weak strain-rate dependency. Only the six-cycle samples showed a statistically significant difference between the strain rates tested. The elastic modulus measured was 1.18 MPa at 45 % strain and at 100 %/s strain rate [45].

Wang and Campbell performed unconfined compressive tests on 3, 5, 15, 25, 35, and 40 % (all wt%) PVA-C samples through 1, 3, and 6 FTCs using a strain rate of 2 mm/min ( $\sim 0.28$  %/s) with strain up to 25 % and temperature of 37 °C to mimic the physiological conditions of intervertebral discs in the lumbar section. The

Young's moduli were measured at 5 and 20 % strain. They found that the Young's modulus increased with an increase in strain, PVA-C concentration, and number of FTCs. The Young's modulus measured was between 0.001 and 2.117 MPa at all combinations of concentration, FTCs, and strain level [54].

Duboeuf et al. reported unconfined compression tests on 10 % PVA-C samples through 2–5 FTCs using a strain rate of 5 mm/min ( $\sim 0.45$  %/s) with strain up to 8 % at room temperature ( $22 \pm 2$  °C). They found that the stress–strain curves were linear and that the Young's modulus increased with the number of FTCs. The Young's modulus, measured between 3 and 8 % strain, was found to range from 0.065 to 0.167 MPa from two to five cycles. The authors also measured the stability of the Young's modulus over a 7-month period. For cycles 2 and 4, the authors found that the Young's modulus did not change significantly. However for cycles 3 and 5, there was a slight increase [55].

Nishinari, Watase, and coworkers studied the effect of degree of polymerization (DP) on the strength of PVA-C. They performed dynamic mechanical analysis on PVA-C samples of seven DPs (ranging from 470 to 17,900 of cycle 1) and of different PVA concentrations. The storage Young's modulus  $E'$  and the mechanical loss of the samples were measured using a 2-Hz excitation strain and at a temperature range of 2–85 °C at a rate of 2 °C/min. The authors found that the storage Young's modulus  $E'$  increased with concentration, and the same  $E'$  value could be obtained at lower concentration by increasing the DP [56]. In addition to the results outlined above, there were several other related studies that reported similar results [20, 57].

Based on the findings of the above papers, all concluded that the unconfined compressive Young's modulus of PVA-C is dependent on the strain, strain rate, DP of PVA, concentration of PVA solution, and the number of FTCs. The Young's modulus reported falls in the range 2–20 MPa, depending on the chosen composition, processing parameters, and the testing conditions used.

The compressive strength of PVA-C can be greatly enhanced by pre- and post-gelation processes such as solvent dehydration and thermal annealing; however, these treatments will significantly reduce the water content of the PVA-C and its lubricating properties, which is undesirable for cartilage and other orthopedic applications. Bodugoz-Senturk et al. introduced a method to counteract this effect by adding poly(ethylene glycol) (PEG) and poly(acrylamide) (PAAm) to PVA, creating PVA-PEG theta gels and PVA-AAm hydrogels [58]. Unfortunately, instead of reporting improvements in compressive strength, they reported improvements in creep resistance.

### 3.1.2 Stress Relaxation and Creep

Stress relaxation characterizes how viscoelastic materials relieve stresses over time under a constant strain. Creep characterizes how viscoelastic materials deform slowly over time under constant stress. Both stress relaxation and creep are typically measured using the normalized value (stress or strain) versus time curve after stress or strain is applied at time zero.

Stammen et al. measured the stress relaxation curves for 20 and 25 % PVA-C by applying a 20 % constant strain and monitoring the stress relaxation for 24 h. They did not report the normalized stress-relaxation curves, instead they plotted the stress (in MPa) variation over time [53].

Millon et al. studied the stress relaxation properties of 10 % PVA-C after 6 FTCs by applying a 45 % constant strain and measuring the normalized stress relaxation for 1 h. They observed that the stress remaining after 1 h did not completely level off [45].

Wang and Campbell studied the stress relaxation curves for their samples by applying a 25 % constant strain and measuring the normalized stress relaxation for 30 s. They also performed creep measurement. The initial load was applied by compressing the samples at 4 mm/s (~33 %/s) up to 25 % strain or when it reached 223 N and holding the force for 30 s [54].

Wong performed creep measurements on 10, 15, and 20 % PVA-C of cycle 6 by applying a constant stress of 0.05 MPa over 1 h. The test was done in phosphate-buffered saline. She found that the samples did not relax completely after 1 h and that increasing the PVA concentration decreased the amount of creep [23].

Due to the biphasic nature and microporous structure of PVA-C, when it is under compression, fluid will flow out of the PVA-C structure gradually until the hydrostatic pressure reaches equilibrium with the external load. This explains the observed results that, as the concentration of PVA increases, the available water content decreases and the stress relaxation and creep effect decrease [23, 51, 53]. For the rate of stress relaxation, both Millon et al. [45] and Wong [23] found that after 1 h the PVA-C had relaxed to 45 % of its initial value but the relaxation still continued. Stammen et al. reported that the relaxation had attained equilibrium after 24 h [53].

### 3.1.3 Tensile

In many biomedical applications in the soft tissue environment or as soft tissue replacement, such as the cardiovascular system, the material will experience stress in tension. Knowledge of the tensile properties of PVA-C is therefore essential for its consideration for use in such physiological environments. The tensile properties of PVA-C have been measured by numerous research groups in the past. Typically, the properties are measured using a material testing system. The test is performed in deionized water or a buffer solution at room temperature or 37 °C. Tensile properties are found to be affected by the average molecular weight or degree of polymerization and concentration of the PVA used, the number of FTCs the samples have undergone, the strain and strain rate employed, the post-hydration period, and the temperature and solution the samples are tested in. The resulting stress-strain curves have a typical “J” shape, are nonlinear, and very similar to those of soft-tissues.

Wan et al. researched into using PVA-C to mimic the tensile properties of the porcine aortic root and evaluated the feasibility of fabricating a stent prototype for

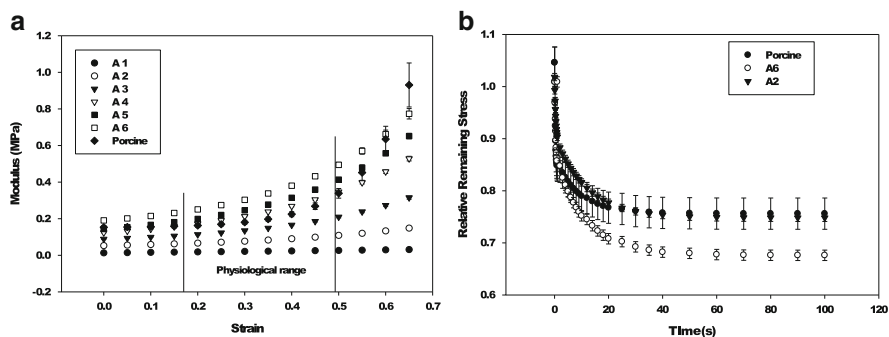


**Fig. 4** (a) Tensile stress–strain curves of 15 % PVA-C through 1–6 FTCs (series A) in comparison with porcine aortic root. (b) Comparison of stress-relaxation properties of 15 % PVA-C of cycles 2 (A2) and 6 (A6) with porcine aortic root. Processing conditions of PVA-C: freezing rate 0.2 °C/min; thawing rate 0.2 °C/min; holding time at +20 °C 6 h; holding time at –20 °C 6 h. Reprinted from [7] with permission. Copyright © 2002 Wiley Periodicals

the bioprosthetic heart valve [7]. They subjected PVA solution with 15 wt% to 1–6 FTCs with a hold time of 6 h at –20 °C and thawing rate of 0.2 °C/min. The samples were tested under a constant strain rate of 40 mm/s (~200 %/s) to a maximum of 80 % strain at 37 °C. In addition, the samples were also subjected to stress-relaxation tests at 80 % strain held constant for 100 s. Figure 4a shows one of the results obtained from their tensile test experiments. It shows the typical J-shaped curves of the stress–strain characteristics of PVA-C in comparison with those of porcine aortic roots. Figure 4b shows the stress-relaxation results. The authors concluded that the variations in holding time at –20 °C had no significant effect on the tensile properties of PVA-C and that the slower thawing rate improved the tensile properties but did not affect the relaxation properties. The authors also determined that the stress–strain curves of 15 wt% PVA-C at cycle 4 best matched those of the porcine aortic root at 17–49 % strain. The typical Young’s modulus was about 350 kPa at 120 mmHg pressure.

Millon et al. developed techniques to fabricate anisotropic PVA-C by applying an initial strain to the PVA samples in a given direction after they had undergone one FTC. The strain was held during subsequent FTCs. This resulted in an increase in the stiffness (Young’s modulus) of the sample in the direction (longitudinal) of the applied strain. In the orthogonal (perpendicular) direction, stiffness remained comparable to the isotropic control sample. The direction in which an initial strain was applied resulted in a higher tensile strength than in the perpendicular direction. As soft tissues are typically anisotropic, the PVA-C fabricated using this technique provides a better matching of soft tissue properties than typical isotropic PVA-C. Figure 5a shows the effects on the stress–strain curves in the longitudinal and perpendicular directions of such PVA-C fabricated with an initial 25 % strain applied in the longitudinal direction, in comparison with a sample with no initial strain applied during the FTC. Figure 5b shows the effects on the Young’s modulus of the resulting PVA-C with different initial strains applied during the FTCs [59].

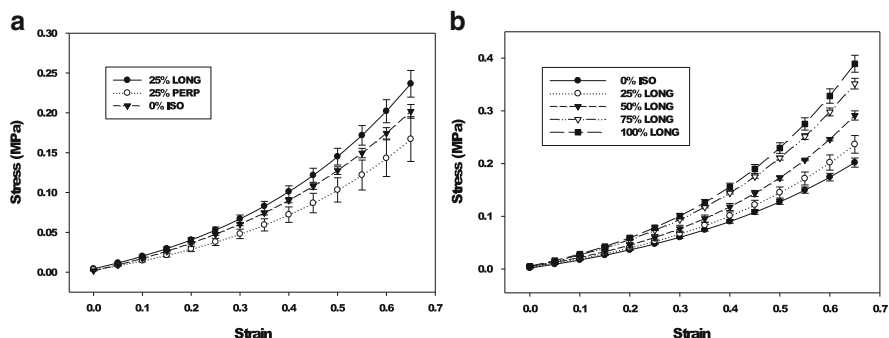


**Fig. 5** (a) Stress–strain curves at the longitudinal and perpendicular direction of an anisotropic 10 % PVA-C of cycle 6 with an initial 25 % strain applied in the longitudinal direction during the FTCs. (b) Effects of variation of initial strains applied to PVA-C during the FTCs. Reprinted from [59] with permission. Copyright © 2006 Wiley Periodicals

Typically, tensile properties are measured using material testing machines, but Fromageau et al. developed a method to measure the tensile properties of PVA-C using four ultrasound elastography techniques. The authors measured the Young’s moduli of 10 wt% PVA-C samples that had gone through 1–10 FTCs using this technique and compared the results with those obtained from tensile testing machines. Good correlations were obtained for samples from cycle 1 to cycle 6 [60].

### 3.2 Diffusion Characteristics

The porous structure of PVA-C, comprised of crystalline regions (~3 nm) and amorphous regions (~19 nm) [10], allows for diffusion of molecules from the cryogel matrix. Work reported by Stauffer and Peppas showed that the water diffusion coefficient decreased as the number of FTCs increased [37], with a diffusion coefficient decrease of 62 % occurring between the second and fifth FTC.

Hickey and Peppas showed that diffusion of solutes from a PVA cryogel membrane is related to the mesh size, which is roughly related to the percentage crystallinity. Also, there is a size exclusion phenomenon present as a result of the presence of the crystallite network. The solute diffusion coefficient for theophylline and FITC-dextran was determined to be dependent on the mesh size [61].

Release of protein (bovine serum albumin, BSA) molecules from PVA cryogel nanoparticles was studied by Li et al. [62]. The authors found that the release was diffusion controlled and that approximately 95 % of the total incorporated protein was released within 30 h. Furthermore, BSA remained stable during the preparation process. It was shown that diffusion increased as temperature increased, and decreased as the number of FTCs increased from one to three. These observations

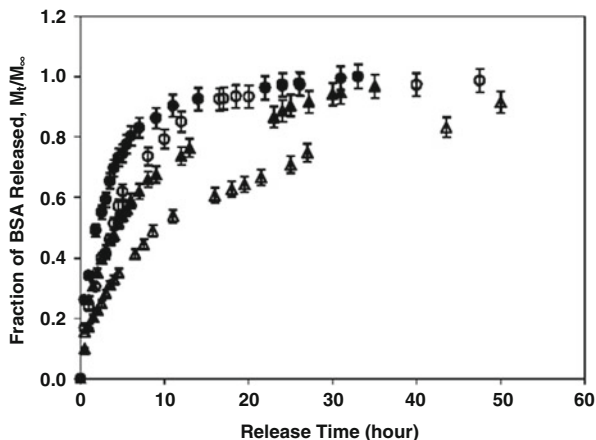


**Fig. 6** Release profiles of BSA from PVA hydrogels subjected to 1 (*filled circle*), 2 (*open circle*), 3 (*filled triangle*), and 6 (*open triangle*) FTCs. These hydrogels were composed of 10 % (w/w) PVA, 0.10 % (w/w) BSA. The freezing and thawing rates were both at 0.50 °C/min

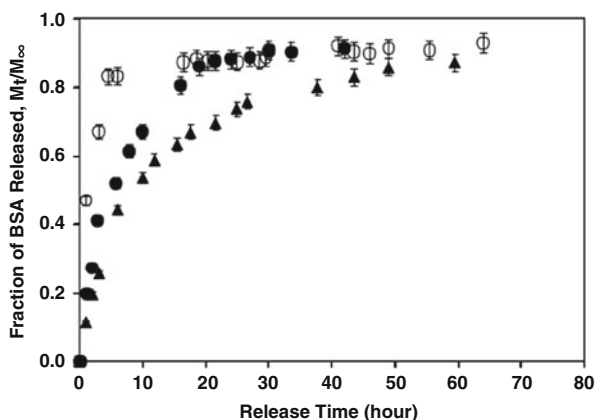
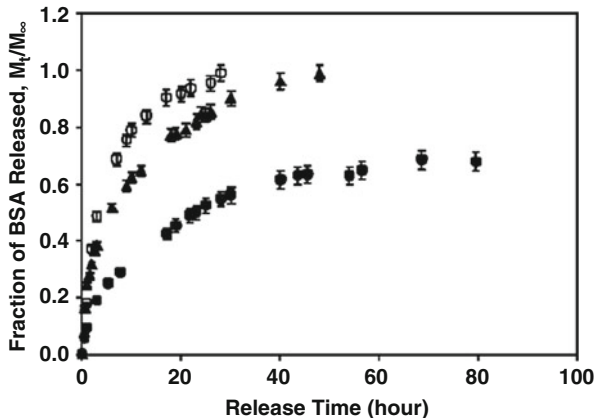


**Fig. 7** Effect of thawing rate on the release of BSA from the PVA hydrogels subjected to two FTCs. These hydrogels were prepared using a fixed freezing rate of 0.10 °C/min and varying thawing rate of 1.00 (*open circle*), 0.25 (*filled circle*), and 0.10 °C/min (*filled triangle*). These hydrogels contained 10 % (w/w) PVA and 0.10 % (w/w) BSA

are consistent with what is known about the PVA matrix structure and the effects of changing the processing parameters [62]. Building on these results, a comprehensive and systematic study was undertaken by our group to provide a global view of the effect of processing (number of FTCs, freezing rate, thawing rate) and composition (PVA concentration) parameters on protein release. PVA-C films prepared by freeze–thaw cycling were used as model drug delivery vehicles with BSA as the model protein. The results are summarized in Figs. 6, 7, and 8. Consistent with the

**Fig. 8** Release profiles of BSA from PVA hydrogels composed of varying concentrations of PVA at 8 (open circle), 10 (filled triangle), and 15 % (w/w) (filled circle). The hydrogels contained 0.50 % (w/w) BSA and were subjected to two FTCs at a constant freezing and thawing rate of 0.10 °C/min



earlier study, it was found that BSA release was mainly by means of a diffusion mechanism. The diffusion coefficients of BSA could be controlled over a 20-fold range by adjusting the processing parameters, including the number of FTCs, PVA concentration, and freezing and thawing rates.

Increasing the number of thermal cycles decreases the release rate (Fig. 6). Every thermal cycle after the first FTC resulted in an increase in the local PVA concentration in the polymer-rich regions concomitant with an increase in the volume fraction of the crystalline regions [61]. This leads to an increase in the time required for the movement of BSA through the amorphous zones of the polymer-rich region, resulting in the observed decrease in the release rate.

Decreasing the freezing rate also decreases the release rate at constant thawing rate. The effect of changing thawing rate is similar to that of changing freezing rate (Fig. 7). A decrease in the freezing or thawing rate allows more time for the polymer chains to reorganize themselves into ordered domains, resulting in an increase in the volume fraction of crystalline PVA and/or increase in the size of the crystalline domains. This leads to a decrease in BSA mobility in the PVA matrix and thus to a decrease in its release rate.

Increasing the PVA concentration in the PVA-C preparation solution decreases the rate of BSA release (Fig. 8). An increase in PVA solution concentration results in a higher polymer concentration in the polymer-rich region after a fixed number of thermal cycles. This decreases the mobility of BSA, leading to an inverse relationship between PVA solution concentration and release rate.

The BSA release rate can be contrasted to that reported for the mechanical properties of PVA-C prepared under similar conditions. The trend in the BSA release rate as a function of PVA solution concentration and number of thermal cycles is analogous to that reported for the mechanical properties of PVA-C. It is interesting to note that, although freezing and thawing rates have an effect on BSA release rate, the thawing rate has a greater effect than that of the freezing rate. In addition, the effects of these two parameters on the PVA-C mechanical properties are quite different. Decreasing the thawing rate leads to significant increases in the mechanical properties, whereas changing the freezing rate had little or no effect [7, 63, 64].

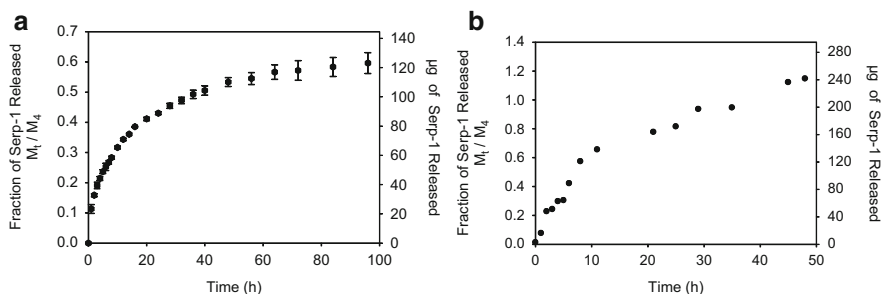


**Fig. 9** (a) Release profile of Serp-1 from PVA-C in a buffer medium. PVA-C samples were prepared using 10 % PVA solution, 0.1 °C/min freezing and thawing rate, two FTCs, and 200  $\mu\text{g}$  Serp-1. (b) Release profile of Serp-1 from PVA-C in human whole blood medium. PVA-C samples were prepared using 10 % PVA solution, 0.1 °C/min freezing and thawing rate, two FTCs, and 200  $\mu\text{g}$  Serp-1. Reprinted from [65] with permission

Although the close parallel between the effects of processing parameters on diffusion and the mechanical properties of PVA-C can be clearly seen, the structural characteristics leading to these observations are quite different. For mechanical properties, the changing stiffness as a function of processing condition is a result of the changing volume fraction of crystalline regions of the material. On the other hand, the diffusion properties are more a function of the properties of the amorphous zone of the polymer-rich regions, largely affected by PVA concentration. Indirectly, the crystalline regions affect the amorphous zone by dictating how tightly the polymer chains are packed, thus making the number of FTCs, freezing rate, and thawing rate contributing parameters to the diffusive properties. Irrespective of the origin of these two observed properties, they could be used to create medical devices with integrated controlled release function, such as the drug-eluting coronary stent, by tuning the mechanical and diffusion properties of the PVA hydrogel simultaneously.

A recent study reports the release profile of the Serp-1 proteinase from PVA-C [65]. Serp-1 is a serine proteinase inhibitor (serpin) secreted by the myxoma virus and is a potential new therapeutic for cardiovascular diseases. It has exhibited anti-inflammatory activity through the modulation of immune cell responses [66]. The release profile of this protein in a buffer medium is typical of that of a diffusion controlled process. However, it is interesting to know that the release rate of Serp-1 and its final release level attained differ in human blood and in buffer. The release rate is twice as fast and in half of the time in blood than in buffer. The final release level is complete in blood and appears to level off at around 50% in buffer. It was suggested that there may be a difference in behavior between the two release media, which is important to consider because human whole blood represents a more realistic setting of the physiological environment in arteries. It is also possible that interaction between PVA-C and blood components play a role in determining the ultimate release rate (Fig. 9a, b) [65].

## 4 PVA Composite Cryogels

PVA-C composites are prepared by the addition of fillers into the PVA solution before the freeze–thaw process. The main purposes of filler addition are for improving mechanical properties and for controlled release and delivery. A wide variety of filler materials that vary in dimensions from micro- to nanometers have been reported, but here we focus on two widely studied filler materials for their relevance in biomedical applications: bacterial cellulose and chitosan.

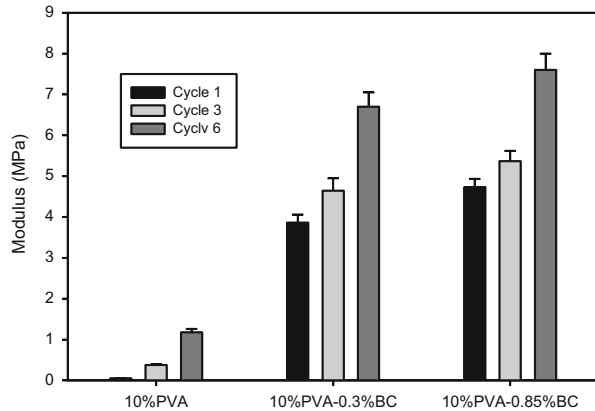
### 4.1 Cellulose-PVA Composites

Bacterial cellulose (BC), a biocompatible natural polymer, has been studied significantly for the production of composite materials for biomedical applications. Its polyfunctionality, hydrophilicity, and biocompatibility [67] make it a desirable material for many different biomedical applications. It is a nanomaterial of roughly 50 nm diameter [68]. Cellulose produced by bacteria has high crystallinity, mechanical strength, the capacity to absorb water, and a large aspect ratio [69, 70]. The use of BC as a composite material for PVA that has been crosslinked using freeze–thaw cycling has so far been limited. The fabrication and use of this composite material with its advantageous properties for biomedical applications will be discussed here.

Wan et al. found that the addition of BC nanofibers to a PVA solution that was then thermally cycled resulted in a PVA-BC composite cryogel that could be tuned to possess the mechanical properties of cardiovascular tissue. BC and PVA-C mimic the role of collagen and elastin, respectively, in soft tissues, making PVA-BC a good candidate material for possible use as a cardiovascular tissue replacement [42]. With the addition of 0.6 wt% BC, the nanocomposite material had higher strength (for FTCs 1–3) and also possessed a broader range of mechanical property control. Because the BC has a very large surface area per unit mass, there is opportunity for significant hydrogen bonding with the PVA matrix, both BC and PVA being hydrophilic polymers. This bonding results in the high strength of the nanocomposite material. The material can be tuned easily by changing processing parameters. Particular compositions of this material were able to show excellent matching with the stress–strain properties of porcine aorta as well as porcine heart valve. Additionally, the material showed faster relaxation and a lower residual stress, which are desirable characteristics for cardiovascular soft tissue replacement applications [42].

The PVA-BC nanocomposite is able to provide a wide range of mechanical properties, depending on the processing parameters chosen for the material's application. As discussed in Sect. 3.1.2, the addition of an initial strain following the first FTC can produce a cryogel with anisotropic mechanical properties. Cardiovascular tissue is composed of the structural proteins collagen and elastin, and is

**Fig. 10** Effect of addition of bacterial cellulose (BC) on the compression elastic modulus of the PVA-BC nanocomposite as a function of the number of FTCs at 45 % strain and 100 %/s strain rate. Reprinted from [45] with permission. Copyright © 2009 Wiley Periodicals



anisotropic with a higher stiffness in the circumferential direction compared to the axial direction [71–73]. For replacement of tissue such as this, or other soft tissue, a composite material that possesses anisotropic properties could be extremely beneficial. Millon et al. prepared PVA-BC samples and found that, compared to the plain PVA system [59], the addition of BC resulted in an almost doubled anisotropic effect, with the overall mechanical properties of the composite material dominated by changes in the longitudinal direction. This is probably due to the fact that the BC crystallites act as nucleation sites during freeze–thaw cycling and therefore promote formation of PVA crystallites around the BC fibers when strain is applied. Stiffness in both directions was found to increase with an increase in the number of FTCs. The anisotropic PVA-BC demonstrated stiffness and relaxation properties very similar to those of the porcine aorta, proving to be an excellent material for potential applications [59].

Following this work, Wan et al. conducted studies on the PVA-BC composite cryogel material for potential use in total joint replacement. In this application, the mechanical properties must be tuned to replicate the properties of the articular cartilage, with its composition of collagen fibrils and proteoglycans. Through compression testing, it was determined that as the number of FTCs increases, the stiffness of the composite material increases. This was consistent with previous results and knowledge. Additionally, stiffness increases with increasing amounts of BC in the PVA matrix. A small increase in weight percent of BC (from 0 to 0.3 %) results in a significant increase in the composite material’s compressive properties. This is shown in Fig. 10. Stress relaxation tests show that the remaining relative stress decreases with an increase in BC concentration. These results are accounted for by the fact that addition of a highly crystalline, hydrophilic BC as a reinforcing biomaterial causes a strong interfacial interaction with the PVA matrix, resulting in significant hydrogen bonding and, thus, creating a stronger material. This could have potential for several biomedical applications [45].

A study conducted by Wang et al. employed the use of PVA-BC produced by freeze–thawing as a composite material for use as an artificial cornea replacement.

The work showed that this composite material is able to achieve similar mechanical properties as the natural cornea and better than pure PVA-C. The composite containing 12 wt% BC had a tensile strength of 3.9 MPa, which is very close to the human cornea tensile strength of about 3.8 MPa [74–76]. Furthermore, the water content of the PVA-BC composites decreases as BC concentration increases. However, composite water content was close to that of the human cornea (78 % [77]) at 67–73 %. Of utmost importance for this application is light transmittance of the material. PVA-BC composite was found to have a high visible light transmittance. Some of the tested compositions actually had a higher transmittance of visible light than pure PVA, due to the nano-effect of the BC nanofibrils. In addition, PVA-BC has good UV absorbance, which is important in preventing damage to internal eye tissue. Overall, this composite material is promising for use as an artificial cornea material [78].

## 4.2 Chitosan-PVA Composites

Another material that has been added to PVA to produce a composite cryogel is chitosan. Chitosan is obtained from chitin by alkaline deacetylation. It is a cationic polysaccharide, and has been proposed as a good material for addition to the PVA matrix for cryogel composite production in order to enhance protein absorption [79]. Due to the hydrophilicity of PVA, cell adhesion proteins are not able to absorb, preventing cell adhesion [79]. Because of this, work to create a more favorable environment for cell growth while still maintaining the beneficial mechanical properties of the PVA cryogel structure is important for certain applications.

PVA cryogels used for vascular tissue engineering scaffolds were modified to improve cell attachment [80]. In this work, chitosan was added to PVA because of its ability to improve vascular smooth muscle and endothelial cell attachment. The blend was subjected to FTCs, immersed in a KOH/Na<sub>2</sub>SO<sub>4</sub> coagulation bath, and the surface modified with collagen type I. The structures were then seeded with bovine aortic vascular smooth muscle and endothelial cells. The presence of chitosan resulted in cell attachment to the surface in patches, which suggests that the regions of high cell density are chitosan-rich and that the other areas are chitosan-poor. Cell attachment and proliferation were shown to increase with an increase in FTCs. Since the coagulation bath treatment essentially eliminates the mechanical difference between samples of different numbers of FTCs, the surface topography is suspected to be responsible for this difference [80].

In another study that focused on the mechanical and morphological properties of PVA-chitosan cryogels, water-soluble chitosan with a deacetylation degree of 85 % (WSC), and water-insoluble chitosan (WIC) were added to PVA separately to produce two different chitosan-PVA cryogel materials, as well as a control plain PVA cryogel. After freeze–thaw cycling, the samples were submerged in a coagulation bath to crosslink the chitosan, because it would not be crosslinked by

thermal cycling, as well as to neutralize the low pH due to the presence of acetic acid. It was found that, again, the number of FTCs has an impact on the mechanical properties. Both WSC and WIC samples demonstrated similar elastic behavior, and the PVA-chitosan samples provided a fairly good replication of the stress–strain behavior of porcine aortic tissue. The macroporous structure was shown to change with the addition of chitosan. For plain PVA, the structure changed visually as the number of FTCs increased, but the change in pore size was not statistically significant after one, two, and four FTCs. When either WSC or WIC was added, the internal structure changed significantly as a function of the number of FTCs. After the second FTC, the pore size increased, and it increased again after the fourth FTC. This study was effective in showing that, although the addition of chitosan may be beneficial for cell adhesion, we cannot ignore the effects that it has on the PVA-C macrostructure and mechanical properties [81].

A system comprised of PVA and chitosan was produced for use as a drug delivery vehicle for the antibiotic sparfloxacin, as well as for use in an antibacterial wound healing device. The addition of chitosan for drug delivery systems can be done to help sustain the release of water-soluble drugs or enhance the availability of water-insoluble drugs. Chitosan also has an intrinsic antimicrobial activity. Different compositions of PVA and chitosan were made and processed through freeze–thaw cycling. Results showed that swelling percentage and gel fraction percentage increased with an increase in chitosan concentration and decreased with an increase in PVA concentration and the number of FTCs. The amount of polymer degraded over a fixed time increased with an increase in chitosan content or a decrease in FTC number. Antimicrobial activity for a variety of Gram-positive and Gram-negative bacteria was tested and it was found that no antimicrobial activity was present at low chitosan percentages but increased as chitosan content increased. Sparfloxacin was added to the chitosan/PVA blend solution before freeze–thaw cycling and its release was determined to be affected by the thickness of the membrane, pH, and temperature of the medium. The total amount of drug released was decreased with an increase in pH due to the presence of  $\text{NH}_2$  within the hydrogel structure that can be ionized at low pH to allow for release. The drug release increased with an increase in thickness and media temperature. This system shows how the addition of chitosan to the PVA cryogel can impart important antimicrobial activity, as well as provide a temperature- and pH-responsive system for drug release [82].

A comparison of composite materials using chitosan, gelatin, and starch added to PVA was reported [79]. A sample for each different component added to PVA was prepared and treated with freeze–thaw cycling and coagulation techniques for application as artificial blood vessels. The resulting mechanical properties were found to be controlled by the PVA rather than by the other components. Each PVA composite sample was found to have similar stiffness behavior to arteries. Increasing the number of FTCs as well as coagulation bath treatment (7.5 % KOH and 1 M  $\text{Na}_2\text{SO}_4$ ) increased the modulus of the hydrogels. Coagulation bath treatment was also shown to increase the resistance of the hydrogel to degradation. Cell adhesion and proliferation studies showed that the addition of a composite material was

beneficial for both cell adhesion and proliferation relative to plain PVA-C. The addition of gelatin was most effective in improving these factors compared to addition of chitosan or starch [79].

## 5 Biomedical Applications

The properties of PVA-C summarized and reviewed thus far demonstrate many of the desirable properties that make it the material of choice for a broad range of biomedical applications. Using the freeze–thaw cycling procedure, PVA-C can be prepared with both tunable mechanical properties and diffusion properties. With the addition of biocompatible nanofillers such as bacterial cellulose and chitosan, the range of these properties can be further broadened. The diffusion properties and some applications of PVA-C for controlled release and delivery have already been covered (see Sect. 3.2). The focus of this section will be on the use of PVA-C as a material for medical devices.

### 5.1 *Medical Devices*

With tunable properties and the ability to create anisotropic orientation-dependent mechanical properties, PVA-C and its composites are suitable candidate materials for medical device application. In this section, we will focus on the use of PVA-C in cardiovascular devices, including vascular grafts and heart valves, and in orthopedic devices, including cartilage and intervertebral discs.

#### 5.1.1 Orthopedic Devices

Orthopedic devices are used for repair and/or replacement in the musculoskeletal system, which is under varying amounts of compressive stress. In considering the use of PVA-C in orthopedic applications, its compressive mechanical properties (discussed in the section on mechanical properties, Sect. 3.1.1.) are the most important parameters to be taken into account.

#### 5.1.2 Intervertebral Discs

Intervertebral discs (IVD) maintain the space between vertebrae. This gap serves as a passageway for spinal nerve bundles to pass through to various parts of the body from the spinal cord. It also allows for motion in the spine, distributes and transfers load to the vertebrae, and provides shock absorption [83]. As humans age, the IVDs degenerate. As a result, some may lose their original thickness or mechanical

integrity. Diseases of the IVD are among the causes of neck and back pain [84, 85] that lead to work absenteeism [86], disability claims [87, 88], and a decrease in the quality of life [89]. IVDs are cartilaginous, composed mainly of collagen and proteoglycans, and have a high water content [84, 90, 91]. They also have low cell numbers and little to no vascularity [84]. Therefore, IVDs have limited ability to heal and regenerate to regain function. The main surgical treatment is to fuse adjacent vertebrae together. However, this approach limits the movement of the patient and effectively shifts the stress to the adjacent vertebrae, developing problems down the road. In recent years, total disc replacement is gaining popularity. The FDA had approved several IVD prosthetic devices. These are mainly made from metal and are typically designed for supporting the bodily load and movements, but with questionable shock-absorbing capabilities. PVA-C prosthesis for IVD total replacement has potential because of its shock absorption capability and biocompatibility.

Wang and Campbell measured the characteristics of PVA-Cs made with varying PVA solution concentrations (3–40 %) and FTCs (1–6) in an attempt to match the mechanical behavior of IVDs based on the Young's modulus, stress relaxation, and creep characteristics under simulated physiological conditions. The authors were only able to match the stress-relaxation and creep characteristic of the IVDs [54].

Instead of total disc replacement, another approach is the replacement or reinforcement of the nucleus pulposus (NP) at the center of the disc with a material that can re-inflate the disc to restore disc height and function. Materials tested include stainless steel ball bearings, polymethylmethacrylate, and silicon, all without much success. More recently, NP implants have been made from cycle-6 cryogels fabricated from a mixture of PVA and polyvinyl pyrrolidone (PVP) with a ratio varying from 1 to 5 % by weight. The implants have been tested and found to better match the physical properties of the NP [92].

Future research efforts in IVD arthroplasty should focus on either partial or full disc functional restoration. This may include NP implants and/or reinforcement or total disc replacement. PVA-C, as a hydrogel, has many interesting properties, such as its long-term biocompatibility and nontoxicity. It is also strongly hydrophilic and viscoelastic with nonlinear stress–strain characteristics similar to the IVD. It has a very low coefficient of friction and has good wear resistance [23]. However, its strength is still too low to serve as a practical functional replacement of the annulus fibrosus. PVA-BC may further increase the strength of the PVA-C to make it a viable candidate material for IVD fabrication.

### 5.1.3 Cartilage

Damaged cartilage can occur from sports or accident-related injuries, as well being a result of degenerative joint disease, which is very common. Total joint replacement is one of the main approaches for treating cartilage degeneration. There is need for a synthetic biomaterial that can mimic the natural cartilage tissue for this purpose. Commonly, ultrahigh molecular weight polyethylene (UHMWPE) is used

as the articular cartilage component, but is not a good match for the mechanical properties. The shock absorption, lubrication, and deformation are inadequate and cause high levels of wear [45]. PVA-C has been studied as a candidate for use as artificial cartilage tissue due to its high water content, viscoelastic properties, and porous structure, all contributing to the resemblance to natural articular cartilage tissue. Furthermore, the natural articular cartilage has been described as possessing biphasic lubrication qualities, which allow movement of fluid away from the contact site over a period of loading. This lubrication, which is intrinsic to natural joint tissue, should be mimicked by artificial replacements [93]. According to Oka et al., the requirements for a good artificial articular cartilage material include good lubrication, sufficient shock-absorbing ability, good biocompatibility, firm attachment to the bones underneath, and high resistance to wear [94].

It was been shown that under both tension and compression, PVA-C displays nonlinear mechanical properties and viscoelastic behavior [95]. Additionally, PVA-C has been observed to have better wear resistance and friction coefficient than UHMWPE [96, 97].

Oka et al. used PVA dissolved in a mixture of water and DMSO to prepare PVA-C and study its properties as artificial articular cartilage. They found that the PVA-C sample allowed a fluid-filled gap, very similar in thickness to the joint space present in natural articular cartilage, to be maintained between the sample and the counter-surface under loading. This is beneficial in maintaining proper fluid film lubrication and weight bearing. In addition, PVA-C displayed a good damping effect by having a lower peak stress value and maintained it for a longer period of time under loading [94].

Articular joints are exposed to compressive forces that are applied very quickly, as well as to very large shear forces. Stammen et al. [53] recognized PVA-C as a viable option for total joint replacement but only if the load-bearing properties could be matched with those of natural tissue. Studies of the compressive tangent modulus and shear tangent modulus were undertaken for the PVA-C product, and a limited strain-rate dependence under unconfined compression was displayed.

Kobayashi et al. were able to use PVA cryogels as an artificial meniscus in animal models. The mechanical properties and viscoelastic characteristics as well as biocompatibility of the material are beneficial for this application. PVA was processed in a DMSO/water solvent, vacuum dried, and heated for annealing. It was then left in water, cut and processed into meniscus form, and used as a prosthesis in rabbits. The samples remained intact for up to 2 years and no fracture or degradation of its mechanical properties occurred. Biocompatibility was also found to be satisfactory [98].

Swieszkowski et al. studied the use of PVA-C as cartilage replacement for the shoulder joint. PVA-C was used as the articular layer of the glenoid component. The mechanical effects of using this material in the glenoid component were evaluated and a model of the cryogel as a hyperelastic material was developed to allow design modifications to limit contact stress [96].

To overcome the issues of limited durability and poor adhesion to tissue, Pan et al. incorporated nano-hydroxyapatite (nano-HA) into the PVA-C matrix

[99]. Nano-HA has been used as a biomaterial for bone repair because it provides bioactive properties and increases adhesion between the natural tissue and composite biomaterial. The nano-HA improves osteoblast adhesion to the biomaterial surface, providing a bioactive bonding interface. The composite material displayed typical viscoelastic properties, with the elastic properties being contributed by the crystalline regions of the PVA and the nano-HA particles, and the viscous characteristics coming from the amorphous PVA regions and incorporated free water. The addition of nano-HA changed the tensile properties of the material by increasing the strength with an increase in HA weight percent, until 4.5 wt%, at which point the strength begins to decrease with an increase in HA content. These trends were accounted for by the increase in interfacial bonding strength between nano-HA particles and polymer matrix, until a certain point at which agglomeration of nano-HA particles reduces the composite strength. The tensile modulus was shown to increase initially with an increase in nano-HA content and then decrease and stabilize due to improved rigidity and decreased degree of crystallinity occurring simultaneously as nano-HA content increased. The effect of elongation and freeze–thaw cycle times on the tensile modulus was studied and it was found that the tensile modulus increased linearly as elongation ratio increased and also increased as FTC time increased. The relationship of tensile modulus and elongation is similar in the composite material and in natural articular cartilage because good deformation ability occurs under low stress conditions. The biomaterial can better withstand high stress conditions due to its higher tensile modulus. These properties are beneficial for a material that must withstand both low and high stress activities, uniformly distribute stress across the tissue, and resist large compressive forces to prevent tissue damage [99].

Another composite material, PVA-BC (described in Sect. 4.1), was studied by Millon et al. as a potential material for cartilage tissue replacement. Bacterial cellulose added to PVA to form a nanocomposite cryogel showed improved strain-rate dependence and good viscoelastic properties for mimicking natural cartilage tissue [45].

Research efforts so far indicate that PVA-C and its composites are promising artificial cartilage replacement materials. Future research efforts should focus on increasing the strength and stiffness of PVA-C. This could be achieved by better-designed nanocomposites. Another challenge is the incorporation of strain-rate dependence properties into the PVA-C material, which are essential for it to withstand high rates of stress changes and function like natural cartilage tissue.

#### 5.1.4 Cardiovascular Devices

Due to the necessity of maintaining blood flow in the cardiovascular system, a positive pressure is always maintained within the system. As a result, tissues making up the system are always under pulsatile tensile stress. In considering the use of PVA-C in cardiovascular applications, its response to pulsatile tensile stress must be taken into consideration. Mechanical property parameters of relevance

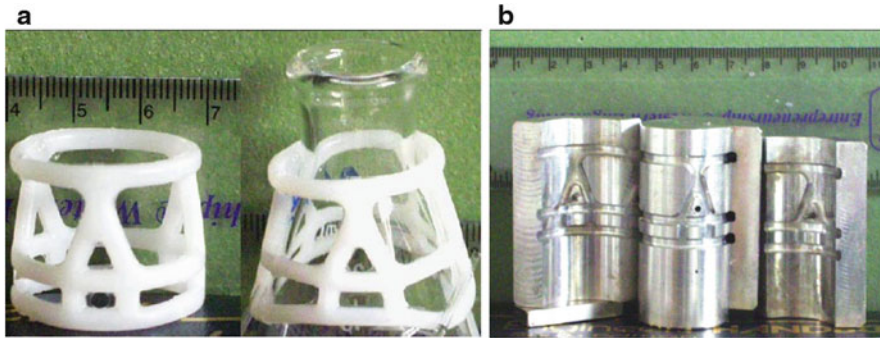


**Fig. 11** (a) PVA-C heart valve stent in natural state and deformed state. (b) Four-part injection mold for the PVA-C heart valve stent. Reprinted from [7] with permission. Copyright © 2002 Wiley Periodicals

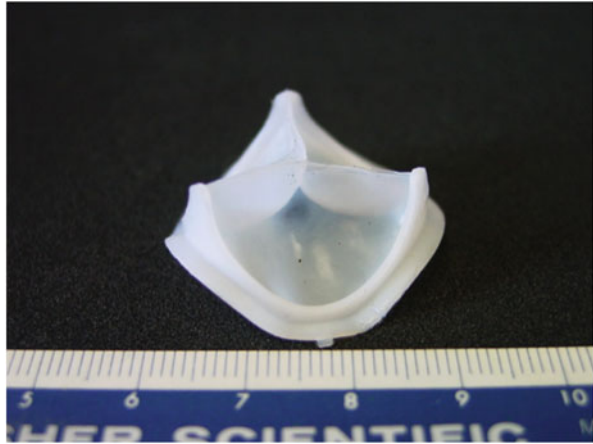
include Young's modulus and stress relaxation properties. These parameters have been discussed in the section on mechanical properties (Sect. 3.1).

The aortic heart valve, which controls the flow of oxygenated blood from the left ventricle into the ascending aorta for distribution to the whole body, is prone to failure. The most common types of artificial replacement are the mechanical and the bioprosthetic heart valves, but they both have shortcomings. One of the early attempts to use PVA-C to alleviate the mechanical problems that can lead to tissue tearing, calcification, and eventual failure of the bioprosthetic heart valve addressed the lack of expansibility of the mounting stent [7]. The PVA solution composition and freeze–thaw cycling processing conditions for the preparation of PVA-C that best mimics the mechanical properties of the porcine aortic root were determined. A prototype heart valve stent was designed and produced using selected PVA-C processing conditions. This study showed that PVA-C can be prepared with tensile and relaxation properties that span a fairly broad range, thus opening the possibility of their use in soft tissue replacement applications (see Fig. 11a, b).

A subsequent study explored the use of PVA-C to produce a one-piece trileaflet heart valve. In this case, a separate heart valve stent is not necessary [100]. A prototype valve was designed and produced using PVA-C (shown in Fig. 12). Using a cyclic flow tester, opening and closing of the PVA-C heart valve prototype was successfully demonstrated. A beneficial property of this design and the choice of PVA-C as the valve material is that the heart valve can be compressed temporarily into a small size so that it can be inserted into the chest cavity through a keyhole incision, thus alleviating the need for open heart surgery [100].

Because natural tissues have anisotropic mechanical properties, in order to better replicate the properties of soft tissue, specifically cardiovascular tissues such as heart valve leaflet and vascular conduits, these anisotropic mechanical properties should be incorporated into the design of PVA-C. PVA-C prepared by the standard freeze–thaw cycling process is isotropic, with mechanical properties independent of sample orientation. Millon et al. [59] produced anisotropic PVA-C by subjecting the hydrogel to an initial controlled unidirectional strain after the PVA solution

**Fig. 12** PVA-C heart valve prototype constructed using the arc subtending two straight lines geometry that integrates into a single part the three leaflets, stent, and sewing ring. Reprinted from [100] with permission. Copyright (2004) Elsevier



underwent the first thermal cycle of the freeze–thaw cycling process [59]. This changed the microstructure of the PVA-C, causing the crystallites to orient in the direction of the stress. Details of the nanostructure of the anisotropic PVA-C have been studied using SANS and USANS [11]. Differences for tensile properties between the longitudinal and perpendicular directions increased as the initial strain applied after the first cycle was increased. The porcine aorta has a higher strength in the circumferential direction than in the axial direction by a factor of 1.75 at a strain of 65 % [42]. These properties are closely matched by the anisotropic PVA-C prepared using three FTCs at an initial strain of 75 %. Finally, stress relaxation tests show that the anisotropic PVA relaxes as fast as porcine aortic tissue and to a lower residual stress, making it a promising material for aortic tissue replacement applications, including heart valves and vascular grafts. Preparation of prototype vascular grafts using the anisotropic PVA-C has been demonstrated [10].

In the process of expanding the mechanical properties range of PVA-C by the creation of the PVA-BC nanocomposite [42], an anisotropic PVA-BC nanocomposite was also prepared using a procedure similar to that for the anisotropic PVA-C [59]. This anisotropic PVA-BC nanocomposite proved to be a material that possesses mechanical properties that closely match those of the porcine aorta, thus making it an attractive material for replacement vascular graft preparation and other cardiovascular applications. The material properties of the anisotropic PVA-BC have been incorporated into the design of a one-piece trileaflet heart valve using a nonlinear finite element modeling method [101].

## 5.2 PVA-C Tissue Hybrid

For medical device application of PVA-C, it is certainly important that its mechanical properties closely match the tissue it is replacing and are compatible with the tissue environment it is implanted into. However, for cardiovascular devices, which

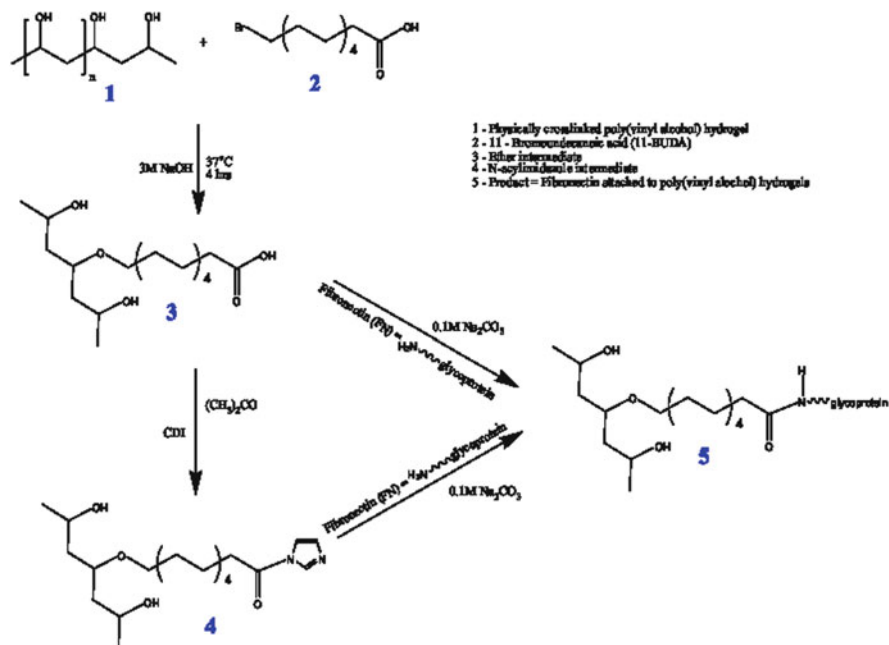


**Fig. 13** Schematic of PVA hydrogels functionalized via fibronectin by two pathways: a simpler route (path 1) works well for PVA-C (1 + 2 → 3 → 5). For chemically crosslinked PVA hydrogels, the route necessary (path 2) requires an additional step involving the reagent carbonyl diimidazole (*CDI*) (1 + 2 → 3 → 4 → 5). Reprinted from [110] with permission. Copyright (2011) Elsevier

have direct blood contact, PVA-C would also have to be hemocompatible. Unfortunately, as with most synthetic materials, PVA is not hemocompatible [102]. One way to overcome this is to create a hemocompatible surface for PVA-C. In vascular tissue, hemocompatibility is provided by a monolayer of vascular endothelial cell on the tissue surface. PVA, being a very hydrophilic polymer, is not conducive to cell adhesion [103]. Many approaches have been tried to promote cell adhesion to the PVA surface with varying degrees of success [79, 104–109]. We have recently reported two approaches that successfully functionalized the PVA-C surface for cell adhesion, including the vascular endothelial cells that are required for hemocompatibility. The resulting material consists of mechanically tuned PVA-C and a living interface of vascular endothelial cells. It can be regarded as belonging to a novel class of “biomaterial–tissue” hybrid materials and, in the present combination of materials, we called it a “PVA-C tissue hybrid”.

In one study [110, 111], the cell adhesion peptide RGD was chemically attached to the PVA-C surface using a more simplified functionalization reaction route than that reported for glutaraldehyde-crosslinked PVA (Fig. 13) and endothelialization was demonstrated on the functionalized surface (Fig. 14). It is interesting that the chemical reactions required for RGD bonding are simpler than those used for

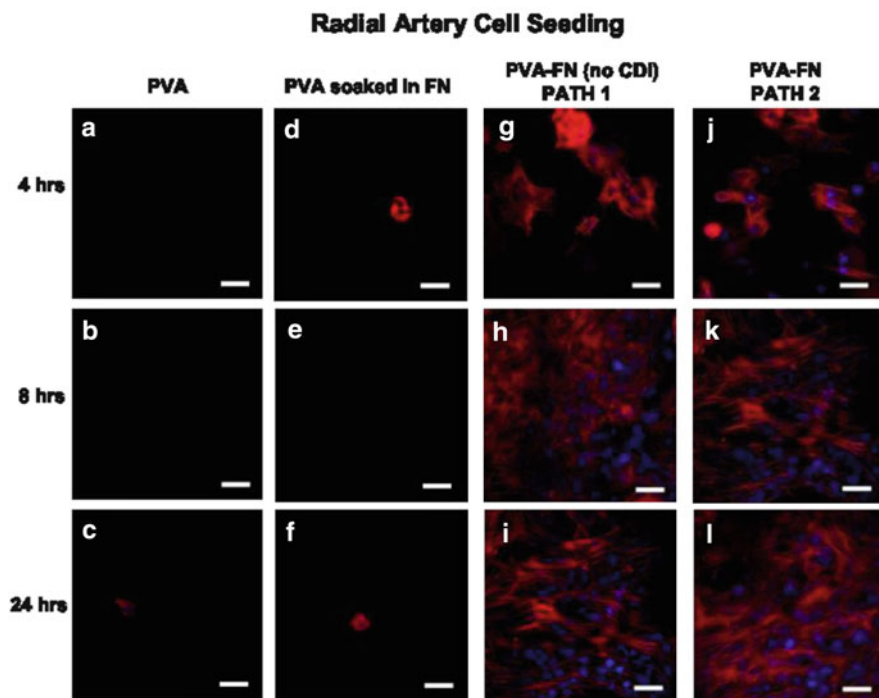


**Fig. 14** Confocal micrographs of radial artery cells seeded onto samples of PVA-C control, PVA-C soaked in fibronectin (FN), PVA-C–FN (FN-functionalized PVA-C) prepared without CDI, and PVA-C–FN prepared with CDI. Cytoskeleton (*red*) was labeled with anti-smooth muscle  $\alpha$ -actin–Cy3-conjugated IgG2a primary. Cell nuclei (*blue*) were labeled with Hoechst 33342. Scale bars: 50  $\mu$ m. For further experimental details, refer to [110]. Reprinted from [110] with permission. Copyright (2011) Elsevier

glutaraldehyde-crosslinked PVA hydrogel. The difference clearly shows the advantage of PVA-C and is attributed to the availability of all the –OH groups for functionalization in PVA-C. In the case of glutaraldehyde-crosslinked PVA, an appreciable fraction of these –OH groups are used for crosslinking and are thus not available for functionalization [110].

Another study aiming to impart cell adhesion properties to PVA-C made use of a recently synthesized novel poly(amic acid) (PAA) polymer that has been shown to be cell compatible to form a PAA-grafted/crosslinked-PVA hydrogel (PAA-*g/c*-PVA). Functionalization of the PVA-C surface was accomplished by grafting of the PAA onto it to provide sites for cell attachment (Fig. 15). Successful endothelization with vascular endothelial cells was demonstrated (Fig. 16) [111].

Both of these approaches are important steps towards the creation of PVA-C tissue hybrids for cardiovascular applications and specifically for heart valves and vascular grafts.

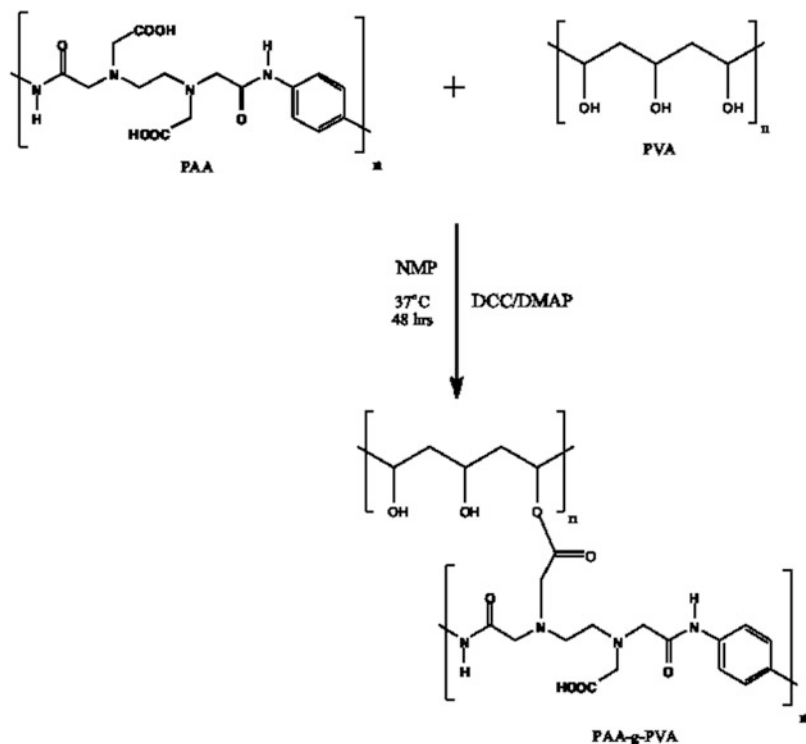


**Fig. 15** PAA-g/c-PVA cryogel synthesis. The reaction requires the use of equimolar amounts of PAA, PVA, and 4-dimethyl aminopyridine (*DMAP*) and an excess of 1,3-dicyclohexyl carbodiimide (*DCC*). Reprinted from [111] with permission. Copyright © 2011 Wiley Periodicals

## 6 Future Perspectives

PVA is a well-known biocompatible material that can be chemically crosslinked into a hydrogel with many demonstrated biomedical applications. When it is physically crosslinked into PVA-C using the freeze–thaw cycling process, the resulting hydrogel (cryogel) possesses additional characteristics such as nontoxicity and tunable mechanical properties. The anisotropic PVA-C has mechanical properties that closely match those of the natural soft tissue, including orientation. These additional characteristics make it an especially attractive candidate material for medical device applications.

For orthopedic devices such as the IVD, the key is to be able to increase the stiffness and strength of the PVA-C. This could be accomplished via PVA-C nanocomposites. In both IVD and cartilage applications, a strain-rate dependent mechanical response is essential. This again may be possible by formulating PVA-C composites with a specially designed filler that can mimic the properties of elastin and proteoglycans in the tissue.

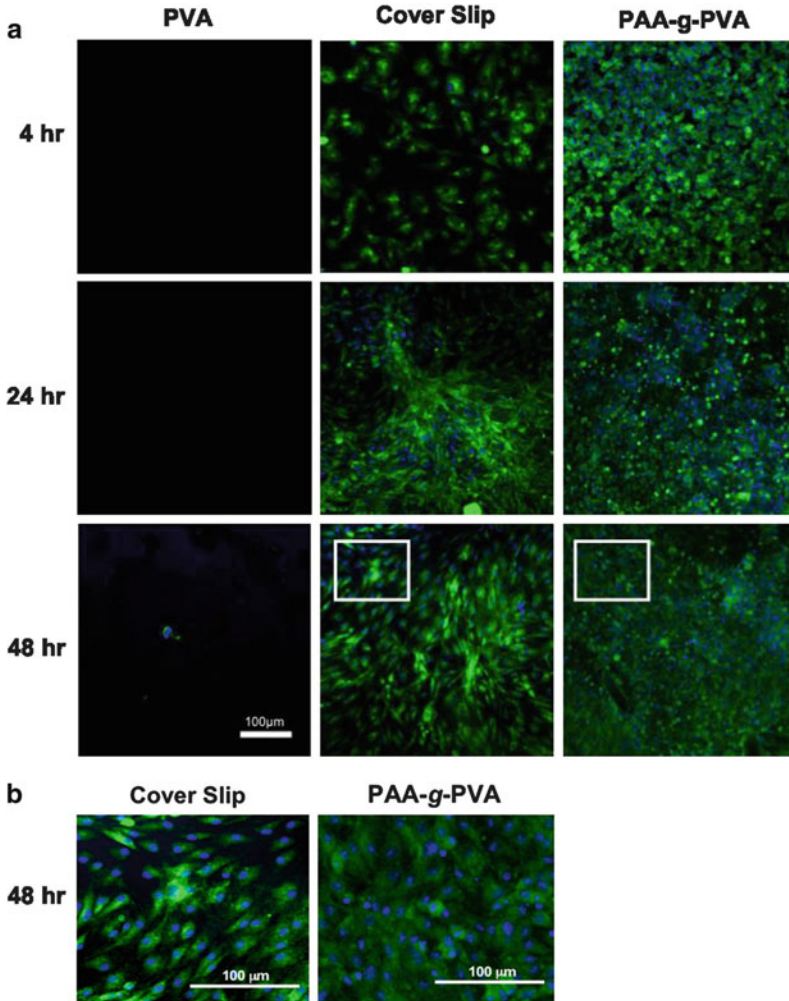


**Fig. 16** (a) Confocal images of endothelial cells at 4, 24 and 48 h on PVA-C hydrogel, on an uncoated (control) coverslip, and on PAA-g/c-PVA. (b) Confocal images of endothelial cells at 48 h on glass coverslips and on PAA-g/c-PVA, focusing on the boxed areas in (a). Cell nuclei (blue) are labeled with Hoechst 33342. Cytoplasmic protein is stained green with the anti-von Willebrand factor. For further experimental details, refer to [111]. Reprinted from [111] with permission. Copyright © 2011 Wiley Periodicals

In cardiovascular devices, it is essential to impart hemocompatibility to PVA-C. The concept of a biomaterial–tissue hybrid in the form of endothelialized PVA-C has been demonstrated. Much work still needs to be done to firmly establish this approach and translate the results into the geometry of a vascular conduit.

Moving ahead, there are certainly challenges facing the use of PVA-C in biomedical applications, but the future looks promising.

**Acknowledgments** This work was supported in part by grants from the Natural Sciences and Engineering Research Council of Canada, the Canadian Institutes of Health Research, and the Canadian Foundation for Innovation.

## References

1. Peppas NA (1996) Hydrogels. In: Ratner BD, Hoffman AS, Shoen FJ, Lemons JE (eds) *Biomaterials science: an introduction to materials in medicine*, 1st edn. Academic, Toronto, ON, Elsevier Academic Press pp 60–64
2. Ratner BD, Hoffman AS (1976) Synthetic hydrogels for biomedical applications. In: Andrade JD (ed) *Hydrogels for medical and related applications*, vol 31, ACS symposium series. American Chemical Society, Washington, DC, pp 1–36
3. Tadavarthy S, Moller J, Amplatz K (1975) Polyvinyl-alcohol (ivalon)—new embolic material. *Am J Roentgenol* 125:609–616
4. Bray JC, Merrill EW (1973) Poly(vinyl alcohol) hydrogels for synthetic articular cartilage material. *J Biomed Mater Res* 7:431–443
5. Peppas N, Benner R (1980) Proposed method of intracordal injection and gelation of poly(vinyl alcohol) solution in vocal cords—polymer considerations. *Biomaterials* 1:158–162
6. Hassan C, Peppas N (2000) Structure and applications of poly(vinyl alcohol) hydrogels produced by conventional crosslinking or by freezing/thawing methods. *Adv Polym Sci* 153:37–65
7. Wan W, Campbell G, Zhang Z, Hui A, Boughner D (2002) Optimizing the tensile properties of polyvinyl alcohol hydrogel for the construction of a bioprosthetic heart valve stent. *J Biomed Mater Res* 63:854–861
8. Yokoyama F, Masada I, Shimamura K, Ikawa T, Monobe K (1986) Morphology and structure of highly elastic poly(vinyl alcohol) hydrogel prepared by repeated freezing-and-melting. *Colloid Polym Sci* 264:595–601
9. Willcox PJ, Howie DW, SchmidtRohr K, Hoagland DA, Gido SP, Pudjijanto S, Kleiner LW, Venkatraman S (1999) Microstructure of poly(vinyl alcohol) hydrogels produced by freeze/thaw cycling. *J Polym Sci Polym Phys* 37:3438–3454
10. Millon LE, Nieh M, Hutter JL, Wan W (2007) SANS characterization of an anisotropic poly(vinyl alcohol) hydrogel with vascular applications. *Macromolecules* 40:3655–3662
11. Hudson SD, Hutter JL, Nieh M, Pencer J, Millon LE, Wan W (2009) Characterization of anisotropic poly(vinyl alcohol) hydrogel by small- and ultra-small-angle neutron scattering. *J Chem Phys* 130:034903
12. Kanaya T, Ohkura M, Kaji K, Furusaka M, Misawa M (1994) Structure of poly(vinyl alcohol) gels studied by wide-angle and small-angle neutron-scattering. *Macromolecules* 27:5609–5615
13. Lozinsky V (2002) Cryogels on the basis of natural and synthetic polymers: preparation, properties and application. *Usp Khim* 71:559–585
14. Holloway JL, Lowman AM, Palmese GR (2013) The role of crystallization and phase separation in the formation of physically cross-linked PVA hydrogels. *Soft Matter* 9:826–833
15. Kanaya T, Ohkura M, Takeshita H, Kaji K, Furusaka M, Yamaoka H, Wignall G (1995) Gelation process of poly(vinyl alcohol) as studied by small-angle neutron and light-scattering. *Macromolecules* 28:3168–3174
16. Ficek BJ, Peppas NA (1993) Novel preparation of poly(vinyl alcohol) microparticles without cross-linking agent for controlled drug-delivery of proteins. *J Control Release* 27:259–264

17. Peppas NA, Scott JE (1992) Controlled release from poly(vinyl alcohol) gels prepared by freezing-thawing processes. *J Control Release* 18:95–100
18. Pazos V, Mongrain R, Tardif J (2009) Polyvinyl alcohol cryogel: optimizing the parameters of cryogenic treatment using hyperelastic models. *J Mech Behav Biomed Mater* 2:542–549
19. Hassan C, Peppas N (2000) Structure and morphology of freeze/thawed PVA hydrogels. *Macromolecules* 33:2472–2479
20. Lozinsky V, Damshkaln L, Shaskol'skii B, Babushkina T, Kurochkin I, Kurochkin I (2007) Study of cryostructuring of polymer systems: 27. Physicochemical properties of poly (vinyl alcohol) cryogels and specific features of their macroporous morphology. *Colloid J* 69:747–764
21. Trieu H, Qutubuddin S (1995) Poly (vinyl alcohol) hydrogels: 2. Effects of processing parameters on structure and properties. *Polymer* 36:2531–2539
22. Millon LE (2006) Isotropic and anisotropic polyvinyl alcohol based hydrogels for biomedical applications. Dissertation, The University of Western Ontario, Canada
23. Wong EYL (2012) Poly(vinyl alcohol) nanocomposite hydrogels for intervertebral disc prostheses. Dissertation, The University of Western Ontario, Canada
24. Hyon SH, Ikada Y (1987) Porous and transparent poly(vinyl alcohol) gel and method of manufacturing the same. US Patent 4,663,358A
25. Ohkura M, Kanaya T, Keisuka K (1992) Gels of poly(vinyl alcohol) from dimethyl sulphoxide/water solutions. *Polymer* 33:3686–3690
26. Lozinsky V, Solodova E, Zubov A, Simenel I (1995) Study of cryostructuring of polymer systems. 11. The formation of PVA cryogels by freezing-thawing the polymer aqueous-solutions containing additives of some polyols. *J Appl Polym Sci* 58:171–177
27. Lozinsky V, Domotenko L, Zubov A, Simenel I (1996) Study of cryostructuring of polymer systems. 12. Poly(vinyl alcohol) cryogels: influence of low-molecular electrolytes. *J Appl Polym Sci* 61:1991–1998
28. Gordon M (1999) Controlling the mechanical properties of PVA hydrogels for biomedical applications. Dissertation, The University of Western Ontario, Canada
29. Shaheen S, Yamaura K (2002) Preparation of theophylline hydrogels of atactic poly(vinyl alcohol)/NaCl/H<sub>2</sub>O system for drug delivery system. *J Control Release* 81:367–377
30. Briscoe B, Luckham P, Zhu S (2000) The effects of hydrogen bonding upon the viscosity of aqueous poly(vinyl alcohol) solutions. *Polymer* 41:3851–3860
31. Nugent M, Hanley A, Tomkins P, Higginbotham C (2005) Investigation of a novel freeze-thaw process for the production of drug delivery hydrogels. *J Mater Sci Mater Med* 16:1149–1158
32. Peppas N, Stauffer S (1991) Reinforced uncrosslinked poly (vinyl alcohol) gels produced by cyclic freezing-thawing processes—a short review. *J Control Release* 16:305–310
33. Hatakeyama T, Yamauchi A, Hatakeyama H (1987) Effect of thermal hysteresis on structural-change of water restrained in poly(vinyl-alcohol) pseudo-gel. *Eur Polym J* 23:361–365
34. Lozinsky V, Plieva F (1998) Poly (vinyl alcohol) cryogels employed as matrices for cell immobilization. 3. Overview of recent research and developments. *Enzyme Microb Technol* 23:227–242
35. Lozinsky VI, Zubov AL, Savina IN, Plieva FM (2000) Study of cryostructuring of polymer systems. XIV. Poly (vinyl alcohol) cryogels: apparent yield of the freeze-thaw-induced gelation of concentrated aqueous solutions of the polymer. *J Appl Polym Sci* 77:1822–1831
36. Lozinsky V, Damshkaln L (2000) Study of cryostructuring of polymer systems. XVII. Poly (vinyl alcohol) cryogels: dynamics of the cryotropic gel formation. *J Appl Polym Sci* 77:2017–2023
37. Stauffer SR, Peppas NA (1992) Poly(vinyl alcohol) hydrogels prepared by freezing-thawing cyclic processing. *Polymer* 33:3932–3936
38. Ricciardi R, D'Errico G, Auremma F, Ducouret G, Tedeschi A, De Rosa C, Laupretre F, Lafuma F (2005) Short time dynamics of solvent molecules and supramolecular organization

- of poly(vinyl alcohol) hydrogels obtained by freeze/thaw techniques. *Macromolecules* 38:6629–6639
39. Holloway JL, Spiller KL, Lowman AM, Palmese GR (2011) Analysis of the in vitro swelling behavior of poly(vinyl alcohol) hydrogels in osmotic pressure solution for soft tissue replacement. *Acta Biomater* 7:2477–2482
  40. Hassan C, Stewart J, Peppas N (2000) Diffusional characteristics of freeze/thawed poly(vinyl alcohol) hydrogels: applications to protein controlled release from multilaminate devices. *Eur J Pharm Biopharm* 49:161–165
  41. Cha WI, Hyon SH, Ikada Y (1993) Microstructure of poly(vinyl alcohol) hydrogels investigated with differential scanning calorimetry. *Macromol Chem Phys* 194:2433–2441
  42. Millon LE, Wan WK (2006) The polyvinyl alcohol-bacterial cellulose system as a new nanocomposite for biomedical applications. *J Biomed Mater Res B* 79B:245–253
  43. Watase M, Nishinari K, Nambu M (1983) Anomalous increase of the elastic-modulus of frozen poly (vinyl alcohol) gels. *Cryo-Letters* 4:197–200
  44. National Toxicology Program (1998) NTP toxicology and carcinogenesis studies of polyvinyl alcohol (CAS no.9002-89-5) in female B6C3F1 mice (intravaginal studies). *Natl Toxicol Program Tech Rep Ser* 474:1–110
  45. Millon LE, Oates CJ, Wan W (2009) Compression properties of polyvinyl alcohol—bacterial cellulose nanocomposite. *J Biomed Mater Res B* 90B:922–929
  46. Watase M, Nambu M, Nishinari K (1983) Rheological properties of an anomalous poly (vinyl alcohol) gel. *Polym Commun* 24:52–54
  47. Fink JK (2011) *Handbook of engineering and specialty thermoplastics, water soluble polymers*. Wiley, Hoboken, NJ
  48. van Aartsen J (1970) Theoretical observations on spinodal decomposition of polymer solutions. *Eur Polym J* 6:919–924
  49. Fergg F, Keil F, Quader H (2001) Investigations of the microscopic structure of poly(vinyl alcohol) hydrogels by confocal laser scanning microscopy. *Colloid Polym Sci* 279:61–67
  50. Ricciardi R, Auriemma F, De Rosa C, Laupretre F (2004) X-ray diffraction analysis of poly (vinyl alcohol) hydrogels, obtained by freezing and thawing techniques. *Macromolecules* 37:1921–1927
  51. Liu K, Ovaert TC (2011) Poro-viscoelastic constitutive modeling of unconfined creep of hydrogels using finite element analysis with integrated optimization method. *J Mech Behav Biomed Mater* 4:440–450
  52. Nakaoki T, Yamashita H (2008) Bound states of water in poly(vinyl alcohol) hydrogel prepared by repeated freezing and melting method. *J Mol Struct* 875:282–287
  53. Stammen JA, Williams S, Ku DN, Guldberg RE (2001) Mechanical properties of a novel PVA hydrogel in shear and unconfined compression. *Biomaterials* 22:799–806
  54. Wang BH, Campbell G (2009) Formulations of polyvinyl alcohol cryogel that mimic the biomechanical properties of soft tissues in the natural lumbar intervertebral disc. *Spine* 34:2745–2753
  55. Duboeuf F, Basarab A, Liebgott H, Brusseau E, Delachartre P, Vray D (2009) Investigation of PVA cryogel Young's modulus stability with time, controlled by a simple reliable technique. *Med Phys* 36:656–661
  56. Nishinari K, Watase M, Tanaka F (1996) Structure of junction zones in poly (vinyl alcohol) gels by rheological and thermal studies. *J Chim Phys Physicochim Biol* 93:880–886
  57. Urushizaki F, Yamaguchi H, Nakamura K, Numajiri S, Sugibayashi K, Morimoto Y (1990) Swelling and mechanical-properties of poly(vinyl alcohol) hydrogels. *Int J Pharm* 58:135–142
  58. Bodugoz-Senturk H, Macias CE, Kung JH, Muratoglu OK (2009) Poly(vinyl alcohol)-acrylamide hydrogels as load-bearing cartilage substitute. *Biomaterials* 30:589–596
  59. Millon LE, Mohammadi H, Wan WK (2006) Anisotropic polyvinyl alcohol hydrogel for cardiovascular applications. *J Biomed Mater Res B* 79B:305–311

60. Fromageau J, Gennisson J, Schmitt C, Maurice RL, Mongrain R, Cloutier G (2007) Estimation of polyvinyl alcohol cryogel mechanical properties with four ultrasound elastography methods and comparison with gold standard testings. *IEEE Trans Ultrason Ferroelectr Freq Control* 54:498–509
61. Hickey AS, Peppas NA (1995) Mesh size and diffusive characteristics of semicrystalline poly(vinyl alcohol) membranes prepared by freezing/thawing techniques. *J Membr Sci* 107:229–237
62. Li JK, Wang N, Wu XS (1998) Poly(vinyl alcohol) nanoparticles prepared by freezing-thawing process for protein/peptide drug delivery. *J Control Release* 56:117–126
63. Gusev D, Lozinsky V, Vainerman E, Bakmutov V (1990) Study of the frozen water poly(vinyl alcohol) system by H-2 and C-13 nmr-spectroscopy. *Magn Reson Chem* 28:651–655
64. Lozinsky VI, Damshkaln LG, Kurochkin IN, Kurochkin II (2012) Study of cryostructuring of polymer systems. 33. Effect of rate of chilling aqueous poly(vinyl alcohol) solutions during their freezing on physicochemical properties and porous structure of resulting cryogels. *Colloid J* 74:319–327
65. Kennedy KL, Lucas AR, Wan W (2011) Local delivery of therapeutics for percutaneous coronary intervention. *Curr Drug Deliv* 8:534–556
66. Richardson J, Viswanathan K, Lucas A (2006) Serpins, the vasculature, and viral therapeutics. *Front Biosci* 11:1042–1056
67. Eichhorn S, Baillie C, Zafeiropoulos N, Mwaikambo L, Ansell M, Dufresne A, Entwistle K, Herrera-Franco P, Escamilla G, Groom L et al (2001) Review: current international research into cellulosic fibres and composites. *J Mater Sci* 36:2107–2131
68. Guhados G, Wan W, Hutter J (2005) Measurement of the elastic modulus of single bacterial cellulose fibers using atomic force microscopy. *Langmuir* 21:6642–6646
69. Klemm D, Schumann D, Udhardt U, Marsch S (2001) Bacterial synthesized cellulose—artificial blood vessels for microsurgery. *Prog Polym Sci* 26:1561–1603
70. Berglund L (2005) Cellulose-based nanocomposites. In: Mohanty AK, Misra M, Drzal LT (eds) *Natural fibers, biopolymers, and biocomposites*. CRC, Boca Raton, FL, pp 819–842
71. Schoen F, Levy R (1999) Tissue heart valves: current challenges and future research perspectives. *J Biomed Mater Res* 47:439–465
72. Fung YC (1993) *Biomechanics: mechanical properties of living tissues*, 2nd edn. Springer, New York
73. Abé H, Hayashi K, Sato M (1996) *Data book on mechanical properties of living cells, tissues, and organs*. Springer, Tokyo
74. Liu W, Merrett K, Griffith M, Fagerholm P, Dravida S, Heyne B, Scaiano JC, Watsky MA, Shinozaki N, Lagali N et al (2008) Recombinant human collagen for tissue engineered corneal substitutes. *Biomaterials* 29:1147–1158
75. Zeng Y, Yang J, Huang K, Lee Z, Lee X (2001) A comparison of biomechanical properties between human and porcine cornea. *J Biomech* 34:533–537
76. Dravida S, Gaddipati S, Griffith M, Merrett K, Madhira SL, Sangwan VS, Vemuganti GK (2008) A biomimetic scaffold for culturing limbal stem cells: a promising alternative for clinical transplantation. *J Tissue Eng Regen Med* 2:263–271
77. Chirila T, Hicks C, Dalton P, Vijayasekaran S, Lou X, Hong Y, Clayton A, Ziegelaar B, Fitton J, Platten S et al (1998) Artificial cornea. *Prog Polym Sci* 23:447–473
78. Wang J, Gao C, Zhang Y, Wan Y (2010) Preparation and in vitro characterization of BC/PVA hydrogel composite for its potential use as artificial cornea biomaterial. *Mater Sci Eng C Mater Biol Appl* 30:214–218
79. Liu Y, Vrana NE, Cahill PA, McGuinness GB (2009) Physically crosslinked composite hydrogels of PVA with natural macromolecules: structure, mechanical properties, and endothelial cell compatibility. *J Biomed Mater Res B Appl Biomater* 90B:492–502
80. Vrana NE, Liu Y, McGuinness GB, Cahill PA (2008) Characterization of poly(vinyl alcohol)/chitosan hydrogels as vascular tissue engineering scaffolds. *Macromol Symp* 269:106–110

81. Mathews DT, Birney YA, Cahill PA, McGuinness GB (2008) Mechanical and morphological characteristics of poly(vinyl alcohol)/chitosan hydrogels. *J Appl Polym Sci* 109:1129–1137
82. Abdel-Mohsen AM, Aly AS, Hrdina R, Montaser AS, Hebeish A (2011) Eco-synthesis of PVA/chitosan hydrogels for biomedical application. *J Polym Environ* 19:1005–1012
83. Causa F, Manto L, Borzacchiello A, De Santis R, Netti P, Ambrosio L, Nicolais L (2002) Spatial and structural dependence of mechanical properties of porcine intervertebral disc. *J Mater Sci Mater Med* 13:1277–1280
84. Adams MA, Roughley PJ (2006) What is intervertebral disc degeneration, and what causes it? *Spine* 31:2151–2161
85. Smith LJ, Nerurkar NL, Choi K, Harfe BD, Elliott DM (2011) Degeneration and regeneration of the intervertebral disc: lessons from development. *Dis Model Mech* 4:31–41
86. Cote P, van der Velde G, Cassidy JD, Carroll LJ, Hogg-Johnson S, Holm LW, Carragee EJ, Haldeman S, Nordin M, Hurwitz EL et al (2008) The burden and determinants of neck pain in workers—results of the bone and joint decade 2000–2010 task force on neck pain and its associated disorders. *Eur Spine J* 17:S60–S74
87. Cote P, Kristman V, Vidmar M, Van Eerd D, Hogg-Johnson S, Beaton D, Smith PM (2008) The prevalence and incidence of work absenteeism involving neck pain—a cohort of Ontario lost-time claimants. *Spine* 33:S192–S198
88. Hoy D, March L, Brooks P, Woolf A, Blyth F, Vos T, Buchbinder R (2010) Measuring the global burden of low back pain. *Best Pract Res Clin Rheumatol* 24:155–165
89. Kovacs F, Abreira V, Zamora J, del Real M, Llobera J, Fernandez C, Kovacs-Atencion Primaria Group (2004) Correlation between pain, disability, and quality of life in patients with common low back pain. *Spine* 29:206–210
90. Cassidy JJ, Hiltner A, Baer E (1990) The response of the hierarchical structure of the intervertebral-disk to uniaxial compression. *J Mater Sci Mater Med* 1:69–80
91. Perie D, MacLean J, Owen J, Iatridis J (2006) Correlating material properties with tissue composition in enzymatically digested bovine annulus fibrosus and nucleus pulposus tissue. *Ann Biomed Eng* 34:769–777
92. Joshi A, Fussell G, Thomas J, Hsuan A, Lowman A, Karduna A, Vresilovic E, Marcolongo M (2006) Functional compressive mechanics of a PVA/PVP nucleus pulposus replacement. *Biomaterials* 27:176–184
93. Northwood E, Fisher J (2007) A multi-directional in vitro investigation into friction, damage and wear of innovative chondroplasty materials against articular cartilage. *Clin Biomech* 22:834–842
94. Oka M, Ushio K, Kumar P, Ikeuchi K, Hyon S, Nakamura T, Fujita H (2000) Development of artificial articular cartilage. *Proc Inst Mech Eng H* 214:59–68
95. Gu Z, Xiao J, Zhang X (1998) The development of artificial articular cartilage-PVA-hydrogel. *Biomed Mater Eng* 8:75–81
96. Swieszkowski W, Ku D, Bersee H, Kurzydowski K (2006) An elastic material for cartilage replacement in an arthritic shoulder joint. *Biomaterials* 27:1534–1541
97. Pan Y, Xiong D, Ma R (2007) A study on the friction properties of poly(vinyl alcohol) hydrogel as articular cartilage against titanium alloy. *Wear* 262:1021–1025
98. Kobayashi M, Chang Y, Oka M (2005) A two year in vivo study of polyvinyl alcohol-hydrogel (PVA-H) artificial meniscus. *Biomaterials* 26:3243–3248
99. Pan Y, Xiong D, Chen X (2007) Mechanical properties of nanohydroxyapatite reinforced poly(vinyl alcohol) gel composites as biomaterial. *J Mater Sci* 42:5129–5134
100. Jiang H, Campbell G, Boughner D, Wan W, Quantz M (2004) Design and manufacture of a polyvinyl alcohol (PVA) cryogel tri-leaflet heart valve prosthesis. *Med Eng Phys* 26:269–277
101. Mohammadi H, Boughner D, Millon LE, Wan WK (2009) Design and simulation of a poly(vinyl alcohol)-bacterial cellulose nanocomposite mechanical aortic heart valve prosthesis. *Proc Inst Mech Eng H* 223:697–711
102. Hui AJ (1998) Hydrogel-based artificial heart valve stent material. Dissertation, The University of Western Ontario, Canada

103. Nuttelman C, Mortisen D, Henry S, Anseth K (2001) Attachment of fibronectin to poly(vinyl alcohol) hydrogels promotes NIH3T3 cell adhesion, proliferation, and migration. *J Biomed Mater Res* 57:217–223
104. Sailaja GS, Sreenivasan K, Yokogawa Y, Kumary TV, Varma HK (2009) Bioinspired mineralization and cell adhesion on surface functionalized poly(vinyl alcohol) films. *Acta Biomater* 5:1647–1655
105. Zajaczkowski M, Cukierman E, Galbraith C, Yamada K (2003) Cell-matrix adhesions on poly(vinyl alcohol) hydrogels. *Tissue Eng* 9:525–533
106. Sugawara T, Matsuda T (1995) Photochemical surface derivatization of a peptide-containing Arg-Gly-Asp (RGD). *J Biomed Mater Res* 29:1047–1052
107. Mansur HS, Costa ES Jr, Mansur AAP, Barbosa-Stancioli EF (2009) Cytocompatibility evaluation in cell-culture systems of chemically crosslinked chitosan/PVA hydrogels. *Mat Sci Eng C* 29:1574–1583
108. Mathews DT, Birney YA, Cahill PA, McGuinness GB (2008) Vascular cell viability on polyvinyl alcohol hydrogels modified with water-soluble and -insoluble chitosan. *J Biomed Mater Res B* 84B:531–540
109. Jiang T, Wang G, Qiu J, Luo L, Zhang G (2009) Heparinized poly(vinyl alcohol)-small intestinal submucosa composite membrane for coronary covered stents. *Biomed Mater* 4:025012
110. Millon LE, Padavan DT, Hamilton AM, Boughner DR, Wan W (2012) Exploring cell compatibility of a fibronectin-functionalized physically crosslinked poly(vinyl alcohol) hydrogel. *J Biomed Mater Res B* 100B:1–10
111. Padavan DT, Hamilton AM, Millon LE, Boughner DR, Wan W (2011) Synthesis, characterization and in vitro cell compatibility study of a poly(amic acid) graft/cross-linked poly(vinyl alcohol) hydrogel. *Acta Biomater* 7:258–267